CHAPTER-II

SYNTHESIS AND CHARACTERIZATION OF POLYMERS

2.1 PREVIEW

Copolymerization is a widely used technique in the production of commercial polymers and also in fundamental investigation of structure property relationship /201/. As the polymer - adsorbent interactions are important in commercial plastics /1/ our interest on the adsorption studies of copolymers and their corresponding homopolymers on various inorganic substrates led to the synthesis of acrylonitrile - acrylate copolymers and homopolymers. Because of high melting point, high melt viscosity and poor thermal stability, polyacrylonitrile (PAN) has limited applications /202/. These deficiencies are tempered by copolymerization. Moreover, PAN fibers are usually produced in the presence of commonomers like methyl acrylate, methy methacrylate, vinyl acetate etc. since the acrylates have low glass transition temperature (Tg) /203-205/, the copolymers are expected to show better processability.

The solution polymerization of acrylic monomers to form soluble polymers or copolymers is an important commercial process, for used in coatings, adhesives, impregnates and laminates /206,207/. These are associated with the adsorption phenomena hence the same technique was used to synthesize the polymers considered for the present study.

Polymer characterization is an essential step in working with the polymers /208/. As discussed in Chapter I knowledge of the polymer characteristics are essential in understanding the adsorption phenomenon. These polymers were characterized by the following techniques :

[1] Elemental Analysis

[2] Infrared Spectroscopy (IR)

[3] ^{13}C NMR

[4] Differential Scanning Calorimetry (DSC)

[5] Differential Thermal Analysis (DTA)

[6] Thermogravimetric Analysis (TGA)

[7] Contact Angle Measurements

[8] Dilute Solution Viscosity

IR absorption spectroscopy is a quick and reliable technique in which energies corresponding to transitions between vibrational and rotational energy states give rise to characteristic patterns. This provides information on chemical, structural and conformational aspects of polymers /209-211/.

Thermo-analytical techniques have become an indispensable tool for polymer characterization /212/. They involve a group of techniques in which properties are measured as a function of temperature or time keeping every other variable constant.

With the development of ^{13}C NMR in the early 1970's the measurement of polymer stereochemical configuration became routine and unambiguous. ^{13}C NMR is superior to ^{1}H NMR, and many studies of polymers using ^{13}C NMR are reported /212-219/. The chemical shift range is larger by about 20 times than that of PNMR, hence the structural sensitivity is enahnced giving rise to well separated resonances for different types of carbon atoms. The low natural abundance of ^{13}C nuclei ($\simeq$ 1%) is another favourable factor. Spin - spin interactions among ^{13}C nuclei can be neglected and proton - ^{13}C interactions are entirely eliminated through hetero - nuclear decoupling. Thus each resonance in ^{13}C NMR spectrum represents the carbon chemical shift of a particular polymer moiety. The microstructure of the polymers which involves the distribution of monomers in the copolymers and the stereochemical arrangement of various groups pendant to the polymer back bone, influences their physical and chemical properties /220/. The ^{13}C NMR sequence determination of acrylonitrile copolymers of methyl methacrylate and ethyl methacrylate were done by Gerken and Ritchey /221/. Microstructure elucidation of Glycidyl-methacrylate (GMA) - alkyl acrylate copolymers by ^{13}C NMR spectroscopy /222/ revealed that the polymerization process was random and GMA was more active than the alkyl acrylates. It was also found that GMA forms steric blocks in the copolymer chains with most units in a syndiotactic mode of arrangement. In this thesis the ^{13}C NMR spectral data are presented for the copolymers of acrylonitrile with methyl, ethyl and butyl acrylates. The corresponding homopolymer spectra are also discussed.

Studies by DSC focus on glass transition measurements and also on specific heat changes in the Tg region, where there is an abrupt energy change. The glass transition is a non equilibrium process and is kinetic in nature /223/. The apparent Tg varies with sample thermal history, rate of cooling and subsequent heating. The sample and the reference material are maintained at an isothermal condition by the required flow of electrical energy, as they are heated or cooled at a linear rate. The heat flow is recorded directly ($\triangle H / \triangle t$) in m cal/sec as a function of temperature in a DSC unit.

In DTA the temperature difference ($\triangle T$) between a sample and a thermally inert material is recorded as both the sample as well as the inert material are heated or cooled at a uniform rate. Temperature changes in the sample are due to endothermic or exothermic transitions /224/ caused by reactions such as phase changes, fusion, boiling, sublimation, vaporization, dehydration, dissociation, decomposition, oxidation, reduction, destruction of crystalline lattice structure etc. In general, phase transitions, dehydration and some decomposition reactions produce endothermic effects, whereas crystallization crosslinking or polymerization, oxidation and other decomposition reactions produce exothermic effects /225/.

Thermogravimetric analysis involves continuous monitoring of the weight of the sample with temperature at a constant rate of change of

temperature or time, isothermally. The commonest use of TGA is in measuring the thermal and oxidative stability of polymers under working conditions /226/. To yield useful information the sample must evolve volatile products from the parent compound /227,228/. In TGA the shape of the curve depends primarily on the kinetic parameters involved i.e. the reaction order, frequency factor and activation energy. Evaluation of these parameters are important in elucidating the mechanism involved in polymer degradation. The experimental and instrumental variables have a pronounced effect /224/ hence these are to be listed in such studies.

The enormous practical importance of wettability of solids explains the large effort that has been put in recent years for understanding the mechanisms and factors that govern the wetting phenomena. Hence contact angle measurement for surface characterization has drawn the attention of many investigators /230-235/. The critical surface tension for spreading (γ_C) can be defined as "the wettability of a solid surface by noting the lowest surface tension (γ_L) a liquid can have and still exhibit a contact angle θ greater than zero degree on that solid /236/". From contact angle data of judiciously chosen liquids it is possible to calculate the various components of surface tension of a large number of polymers /237-239/. Those components being γ_d (due to dispersion forces), γ_p (due to polar forces), γ_h (due to hydrogen bending)

$$\gamma = \gamma_d + \gamma_p + \gamma_h$$

These data are useful to predict wettability by different liquids and also at a more fundamental level, to the understanding of molecular interactions across an inteface and their relation to the interactions within each individual phase /240/. The contribution from dispersion, polar and hydrogen bonding forces can, be clearly, hence, understood.

Dilute solution viscosity is basically a measure of the size or extension in space of polymer molecules /241/. It is empirically related to molecular weight for linear polymers. The simplicity of measurement and the usefulness of viscosity molecular weight correlation are so remarkable that viscosity measurements constitute an extremely valuable tool for the molecular characterization of polymers in solutions.

2.2 MATERIALS AND METHODS

2.2.1 SYNTHESIS OF POLYMERS

The monomers acrylonitrile, methyl acrylate (Fluka), ethyl acrylate and butyl acrylate (National Chemicals, Baroda, India) were purified to remove stabilizers by washing with 1% NaOH aqueous solution and then with distilled water until free of NaOH. These were then dried over fused calcium chloride, distilled in dry atmosphere and the middle fractions were used. Other solvents, NN' Dimethyl formamide (DMF), acetone and methanol were distilled in dry atmosphere prior to use.

Solution polymerization technique was used for the synthesis of the polymers. The acrylonitrile - acrylate feed ratios were varied to obtain a series of copolymers. They were 1:1, 1:2 and 1:3 (w/w) symbolised as $ANXA_{11}$, $ANXA_{12}$ and $ANXA_{13}$, where XA stands for methyl, ethyl or butyl acrylate and AN for acrylonitrile. The monomers were added to four times quantity of DMF in a round bottom flask. Benzoyl peroxide (1% w/w) was used as the initiator. Nitrogen was purged through this mixture for few minutes and then the reaction was controlled at 85°C with continuous stirring for 6 hours. The product was then precipitated in excess quantity of methanol and dried in vacuo after several washings with methanol. These were then soxhlet extracted with toluene to remove homopolymers of the acrylates, dried and dissolved in acetone. Later reprecipitated in methanol and dried thoroughly over vaccum. Polyacrylonitrile (PAN) being insoluble in acetone the traces of these could be effectively separated. Before taking these samples for analysis they were purified again by dissolving in acetone and reprecipitating with methanol and dried to constant weight under vaccum. The corresponding homopolymers were also synthesized and purified under similar experimental procedures.

2.2.2 CHARACTERIZATION

Nitrogen estimation was done by Dumas method. Infrared spectra of the polymers were recorded on a Shimadzu IR-408 spectrophotometer. The films were prepared by dissolving the polymer in acetone and

pouring the solutions over a pool of mercury. The solvent was vacuum evaporated slowly to obtain transparent films. In case of PAN, KBr pallet was prepared by grinding about 2 mg of the sample with KBr (100 - 150 mg) and compressing the whole into a transparent pellet. KBr was dried at 105°C before using.

^{13}C NMR spectra of the polymers were recorded with a Varian XL - 300 instrument operating at 75 MHz, at the Regional Sophisticated Instrumentation Centre (RSIC), Indian Institute of Technology, Bombay. The acrylate homopolymer spectra were recorded using $CDCl_3$ as the solvent and for PAN and copolymers DMSO - d_6 was used. The internal standard used was TMS. The detail conditions of operations are as follows : temperature of the probe 25°C, pulse width 10μs, pulse delay 0 sec., spectral width 21978 Hz, mode of decoupling, gated. These experimental conditions ensure the complete relaxation of all the ^{13}C carbons. The polymer samples were anlysed as 15-20% (w/v) solutions.

DSC were recorded on a Dupont 2000 thermal analyser in nitrogen atmosphere at Department of Colour Chemistry, Leeds University, Leeds, U.K. and on a Mettler TA 4000 system at Applied Chemistry Departmenbt, M.S. University, Baroda.

TGA and DTA were done on a Shimadzu thermal analyser DT-30B. About 10 mg each of the samples were taken for analysis. Heating rate was maintained at 10°C/min in presence of air.

Contact angle measurements were done with a contact θ meter fabricated at Leeds University, U.K. Contact angle for different liquids were determined at room temperature ($\simeq$ 20°C). Polymer films were cast over mercury using acetone solvent. These films were cautiously transferred onto a smooth glass plate and then placed on the contact θ meter. At least six different liquids with known surface tension values at 20°C from the list in Table 2.1 were used to determine the contact angle.

The contact angle for each system was determined at various points of the surface (atleast 5). The average values were then taken. The standard deviation of the mean was ±2°. The small deviation indicates some amount of heterogeneity on the surface.

The viscosity of the dilute polymer solutions in DMF (the solvent used for adsorption studies) were determined using an Ubbelohde viscometer kept vertically in a thermostatted water bath at all the required temperatures with an accuracy of ±0.05°C. The concentration range of the polymer solution was from 0.2 to 0.8 g/dl. Since the efflux flow time was more than 100 seconds, kinetic corrections were not considered. The density of the solvent (DMF) was measured using a pycnometer at the required temperatures. Since the Mark-Houwink constants for the copolymers are not reported in the literature the value of PAN has been considered to calculate the viscosity average molecular weight (Mv) of the copolymers /242/. For poly (methyl acrylate), poly (ethyl acrylate) and poly (butyl acrylate) also the

TABLE : 2.1

SURFACE TENSION VALUES OF

VARIOUS LIQUIDS

Liquid	γ_L at 20°C mN m^{-1}
Formamide	58.20
Ethylene glycol	47.70
Aniline	41.75
Nitrobenzene	43.90
Sulphuric acid	55.10
Dioxane	32.59
Formic acid	37.60
Water	73.05

Mark - Houwink constants were not reported for DMF solvent systems. Hence the intrinsic viscosity $|\eta|$ was determined using toluene, chloroform and acetone at 35°C, 30°C and 25°C for the respective polyacrylate where the Mark-Houwink constants are known. $\bar{M}v$ values are tabulated in Table 2.2.

2.3 RESULTS AND DISCUSSION

2.3.1 ELEMENTAL ANALYSIS

From the results obtained by Nitrogen estimation, the experimental mole ratios were calculated. The results are compiled in Table 2.2. These results show that the amount of acrylate moiety is less in the copolymer samples than acrylonitrile in the respective feed ratios.

2.3.2 INFRARED SPECTRA

Representative copolymer spectra are shown in fig. (2.1 a,b,c). The spectra shows characteristic bands at 2241 cm^{-1} and 1741 cm^{-1} for -CN and -COOR groups respectively. It can also be seen that a qualitative trend exists when the peak heights corresponding to acrylate and acrylonitrile are compared to the experimental mole ratios of the copolymers.

TABLE : 2.2

SOME EXPERIMENTALLY DETERMINED PARAMETERS FOR THE HOMOPOLYMERS AND COPOLYMERS

Polymer	Percentage Nitrogen content (N%)	Expt. mole. ratio AN : XA	γ_c mNm^{-1}	Viscosity average mol. wt. $\bar{M}_v$* x 10^{-3}	Tg °C
$ANMA_{11}$	11.49	1 : 0.86	37	15.7	58
$ANMA_{12}$	8.05	1 : 1.40	33	13.2	53
$ANMA_{13}$	5.65	1 : 2.27	30	12.6	37
$ANEA_{11}$	12.63	1 : 0.58	34	22.6	57
$ANEA_{12}$	9.25	1 : 0.98	29	18.8	48
$ANEA_{13}$	7.41	1 : 1.36	24	21.0	-
$ANBA_{11}$	11.71	1 : 0.52	30	15.8	55
$ANBA_{12}$	8.51	1 : 0.82	24	15.3	-
$ANBA_{13}$	7.95	1 : 0.96	21	13.8	-
PMA	-	-	-	20.5	-
PEA	-	-	-	21.0	-
PBA	-	-	-	22.1	-
PAN	25.2+	-	-	52.0	-

* K and α values were taken from Reference /242a/.

\+ Theoretical value 26.4.

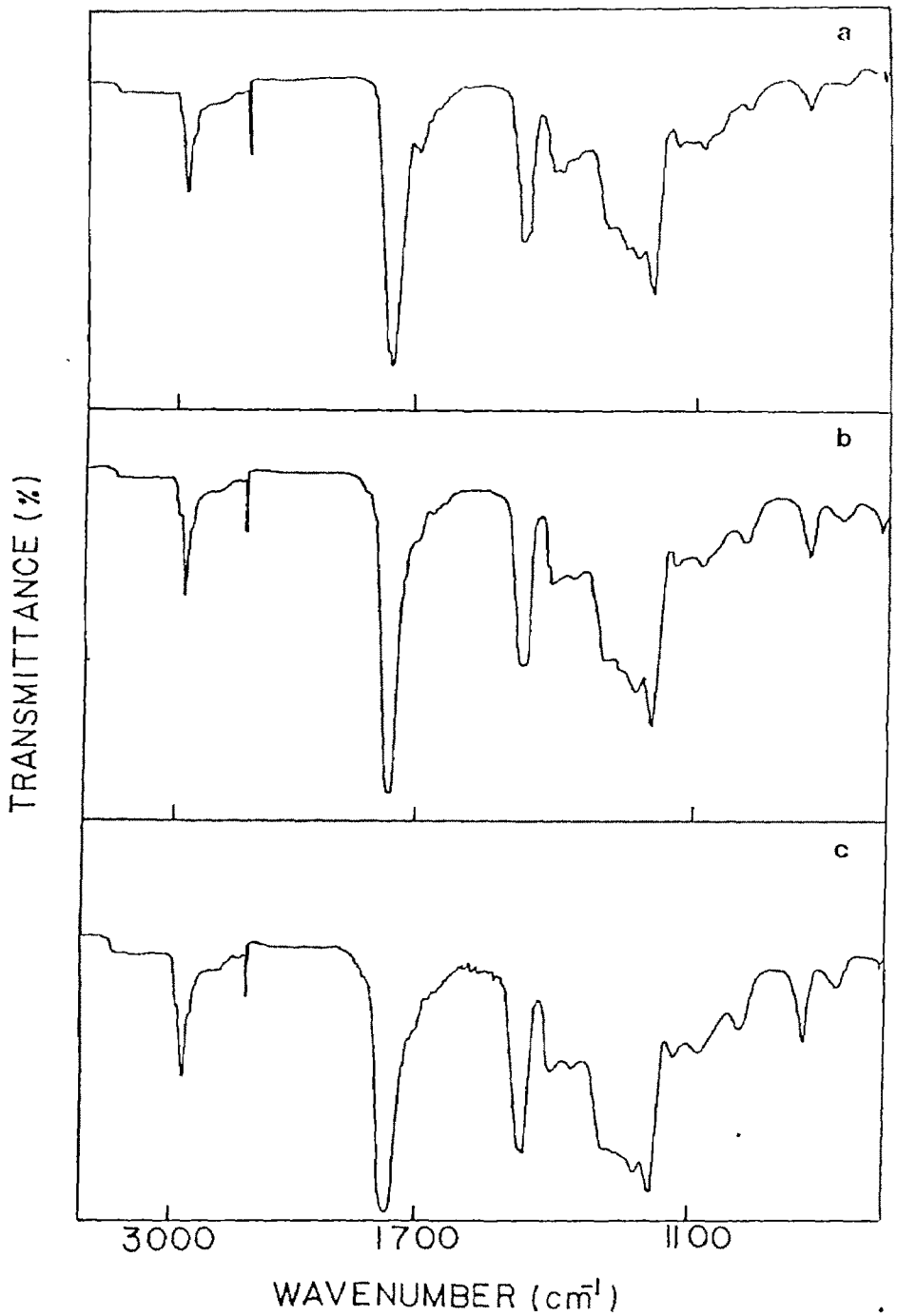

Fig. 2.1 : Infrared spectra of acrylonitrile-acrylate copolymers.
a. $ANMA_{11}$ b. $ANMA_{12}$ c. $ANMA_{13}$

2.3.3 ^{13}C NMR SPECTRA

^{13}C Resonance of homopolymers.

The ^{13}C NMR spectra of poly acrylonitrile, poly (methyl acrylate), poly(ethyl acrylate) and poly(butyl acrylate) are shown in figs. 2.2. to 2.5. The assignment of various resonance peaks, due to different carbon atoms, was made by comparison with the reported spectra and analogous groups from the literature /222,243-245/.

In PAN, the nitrile carbon resonance appears at 120.1 to 120.9 ppm, methylene carbon at 33.0 to 33.3 ppm and methyne carbon at 27.3 to 28.4 ppm. The spectrum matches well with that reported in literature /243/. The relative intensities observed for the triads of nitrile carbon resonance are about 3:4:2.5 and are consistent with increased stereoregularity with the atactic fraction dominant. The three lines have been assigned to iso, hetero and syndiotactic triads in order of increasing field from left to right.

In PMA fig. 2.3 the carbonyl carbon resonance appears at 174.8 ppm, methoxy carbon at 51.6 ppm, methyne carbon at 41.2 ppm and the methyl carbon between 34.8 to 35.9 ppm. These are in agreement with the reported spectra /245/.

In case of PEA and PBA also the observed carbonyl carbon, main chain methylene, methine, methoxy carbon resonances are at the same

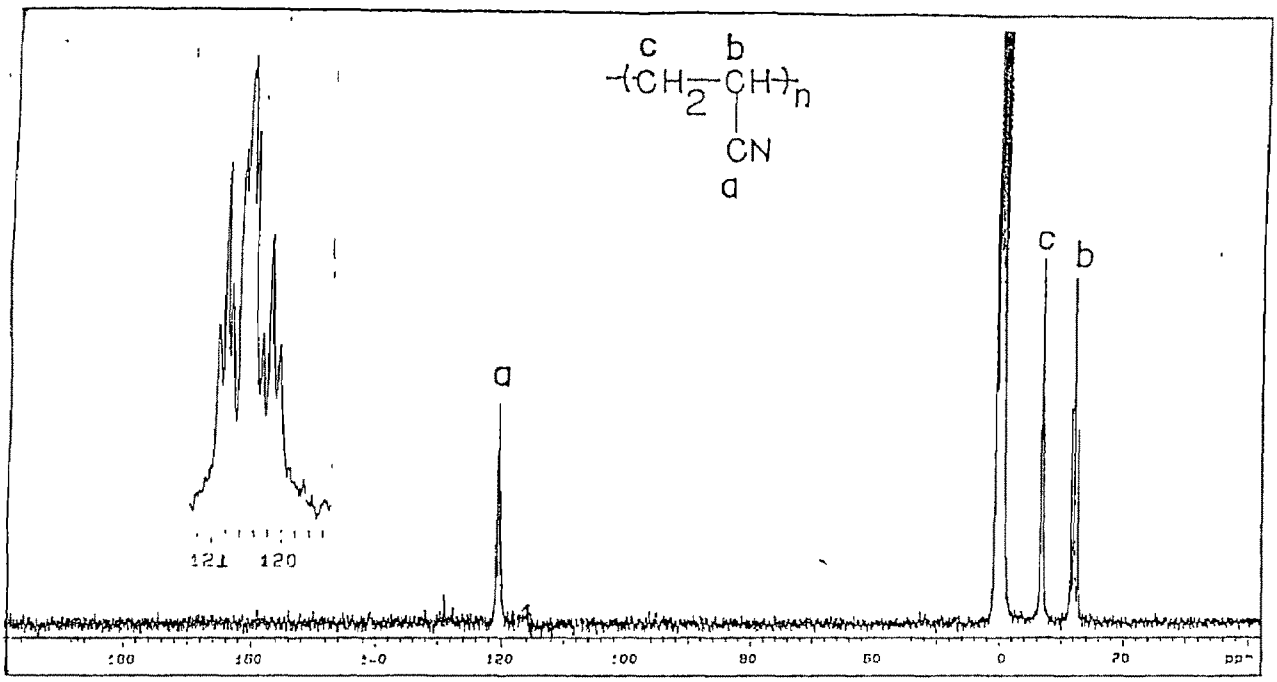

Fig.2.2 ^{13}C NMR spectrum of Polyacrylonitrile .

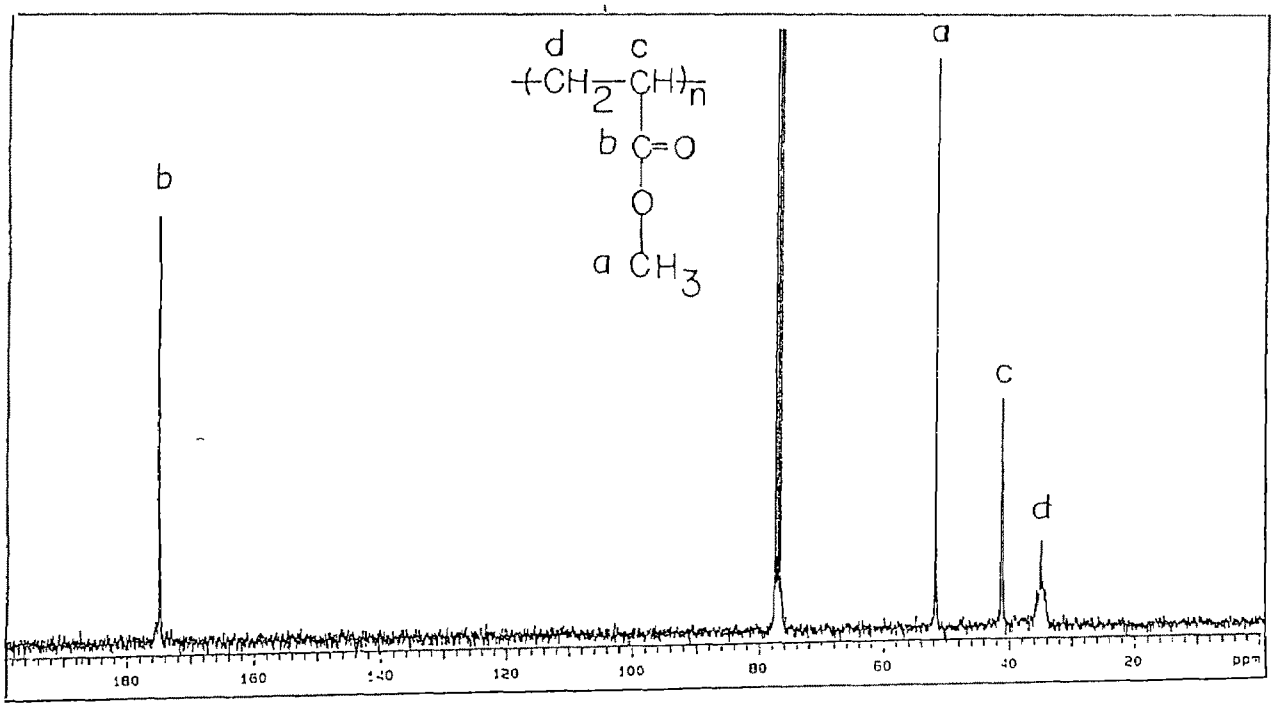

Fig.2.3 ^{13}C NMR spectrum of poly(methyl acrylate).

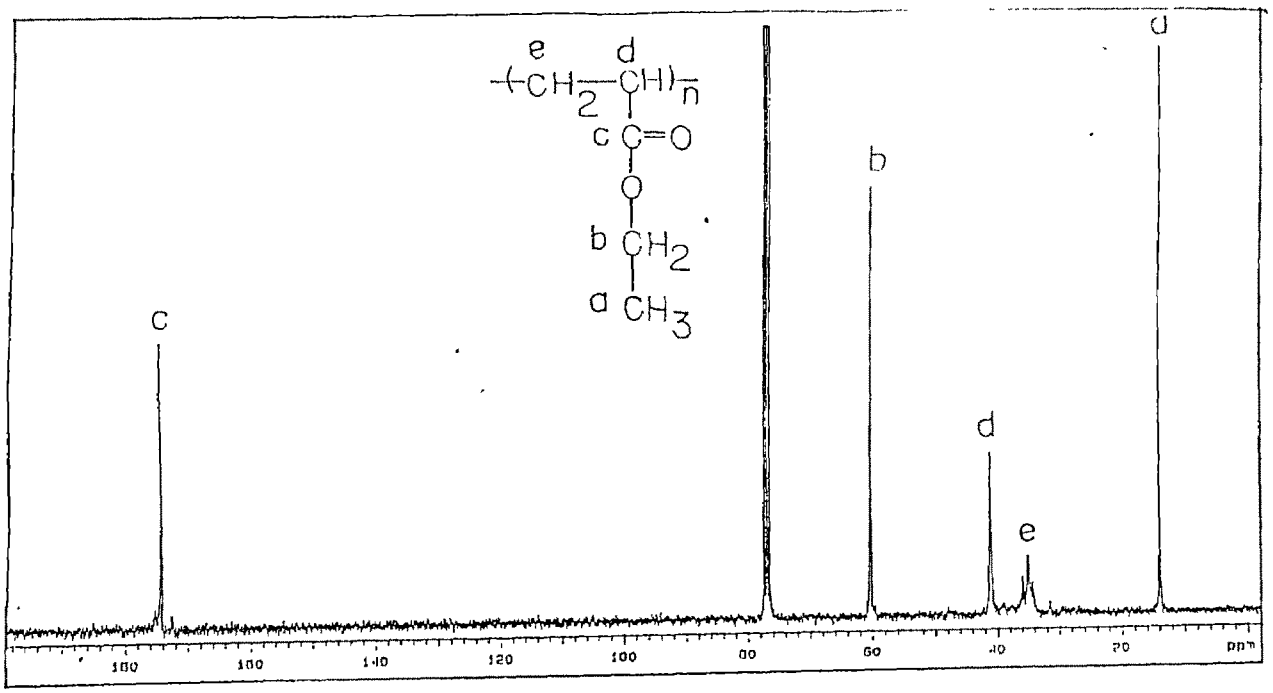

Fig.2.4 ^{13}C NMR spectrum of poly(ethyl acrylate)

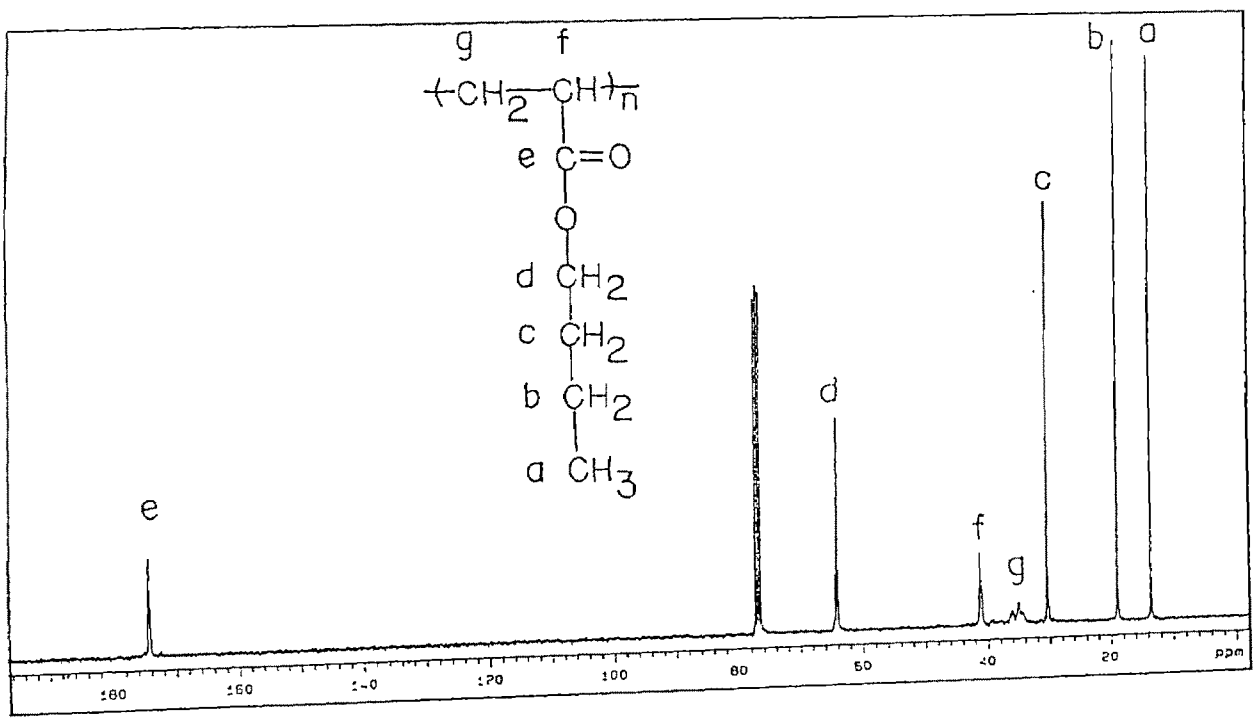

Fig.2.5 ^{13}C NMR spectrum of poly(butyl acrylate)

ppm as in PMA. In PEA the methyl resonance is observed at 14.0 ppm. In the case of PBA the methyl resonce is at 13.5 ppm and matches well with the reported spectra /222/. In all these poly acrylates the carbonyl carbon do not show any Splitting but the methylene carbons show splitting due to configurational effects.

^{13}C Resonances of Copolymers.

The ^{13}C resonance spectra of ANMA, ANEA and ANBA copolymers are shown in fig. 2.6, 2.7 and 2.8 respectively. The assignment of peaks due to various carbon atoms of the copolymer were done by using the corresponding homopolymer spectra.Unlike in the homopolymers of acrylates the carbonyl carbon in all these copolymers shows splitting. Also various spliiting patterns are observed in resonances of back bone methylene, nitrile carbon and the quarternary carbon. The splitting is influenced by the composition of the copolymers and is due to configurational and sequence distribution effects. As a standard was not available at the moment, a quantitative determination of these are not considered. It was observed that with the increasing content of MA, EA or BA (acrylate fraction) in the copolymers there is more tendency towards ordered arrangement, with the isotactic fraction predominant. The intensity of the carbonyl resonance also increases. This diminishes the resolution of nitrile carbon and its intensity. However, the tendency for more ordered arrangement is relatively less in ANBA copolymers with the increasing content of BA. Similar phenomenon has been observed in the copolymers of glycidyl

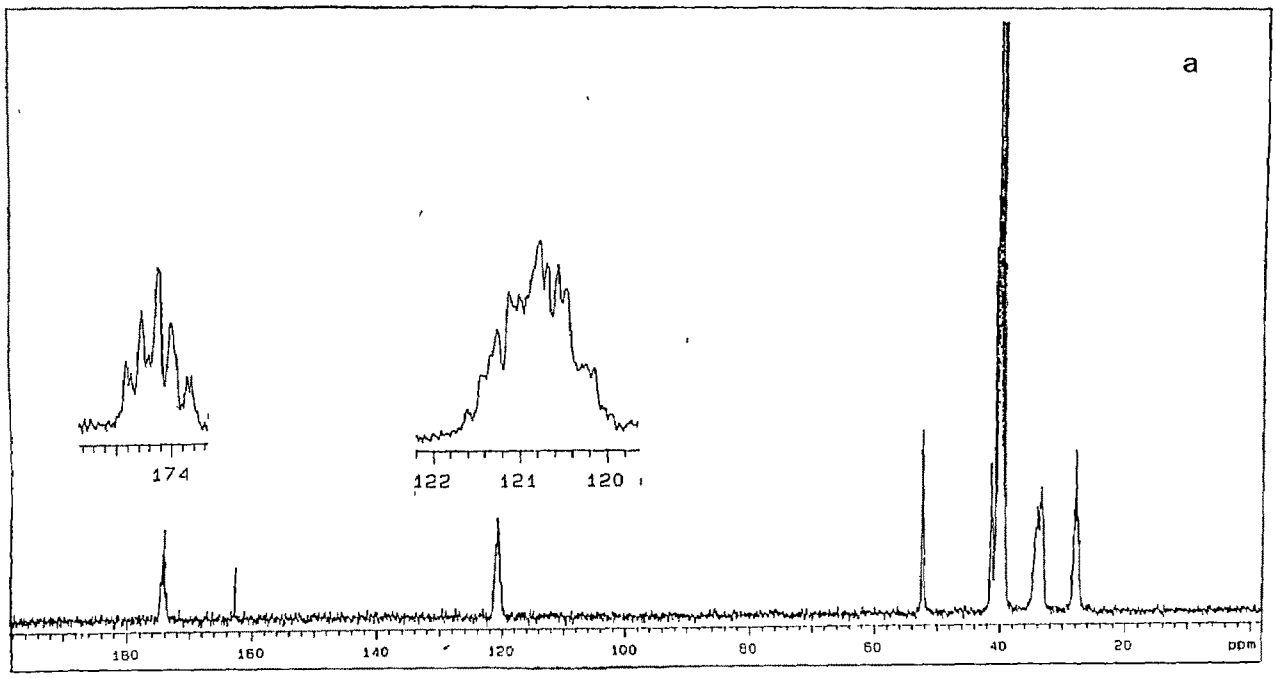

Fig.2.6 a ^{13}C NMR spectrum of $ANMA_{11}$

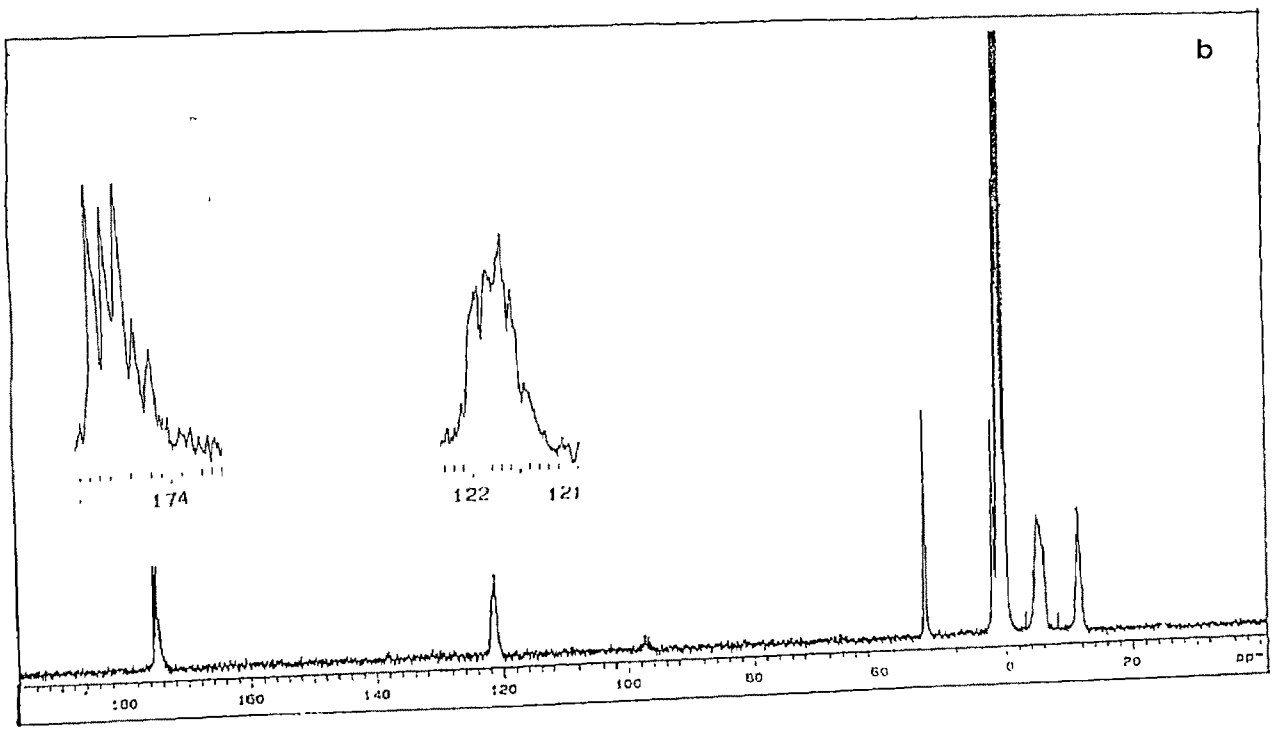

Fig.2.6 b ^{13}C NMR spectrum of $ANMA_{12}$

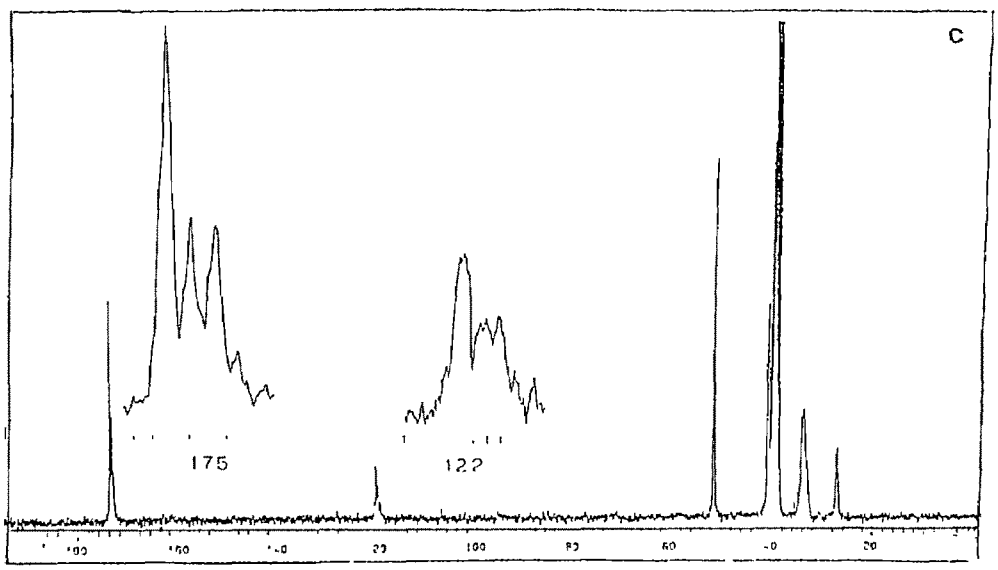

Fig.2.6 c ^{13}C NMR spectrum of $ANMA_{13}$

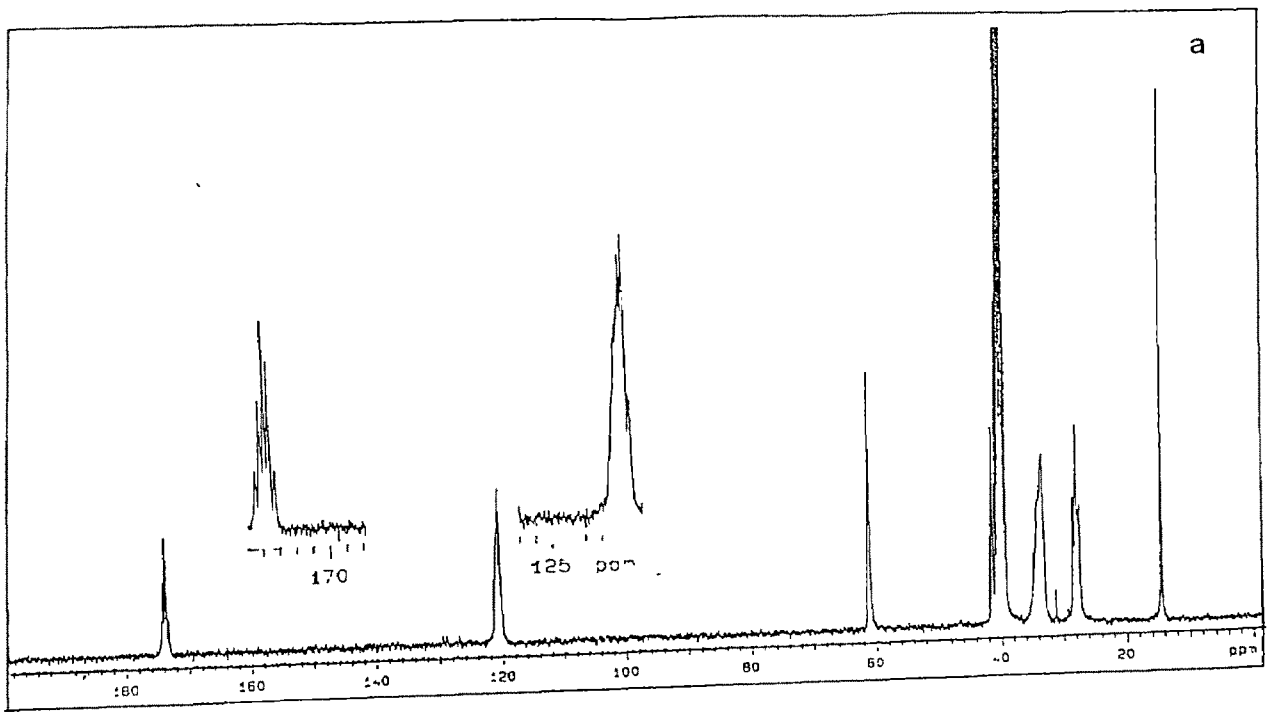

Fig.2.7 a ^{13}C NMR spectrum of $ANEA_{11}$.

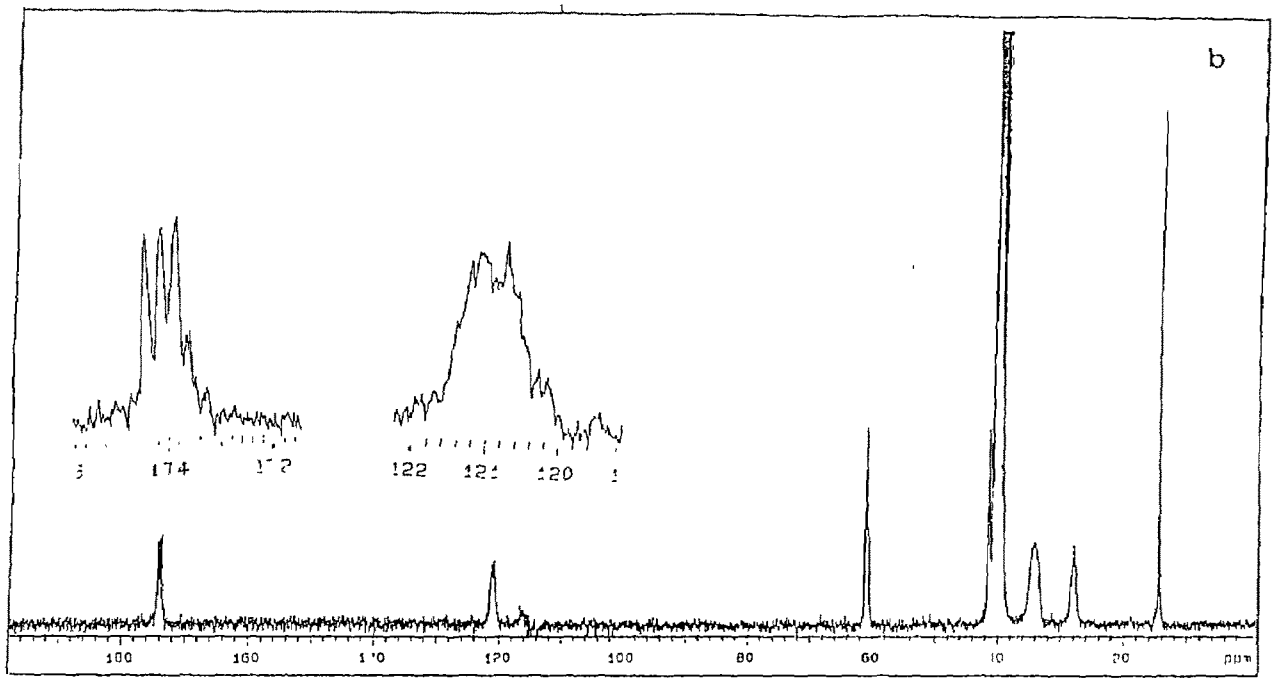

Fig.2.7 b ^{13}C NMR spectrum of $ANEA_{12}$.

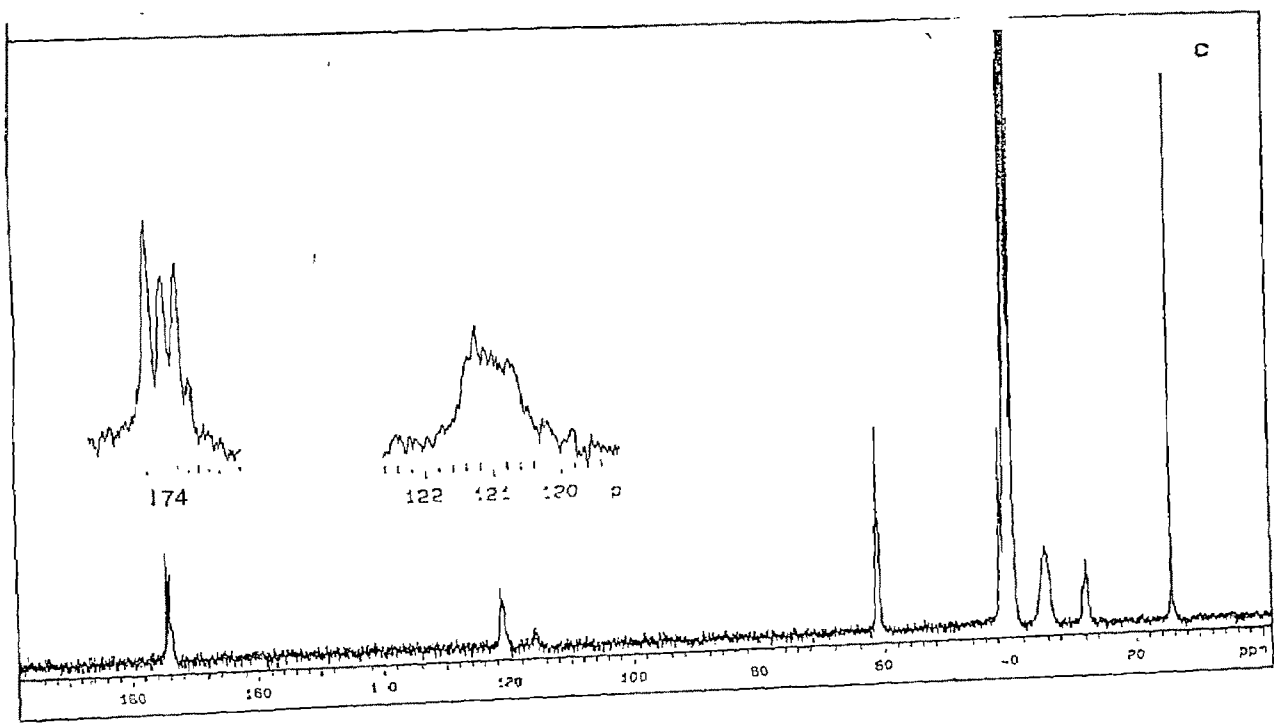

Fig.2.7 c ^{13}C NMR spectrum of $ANEA_{13}$

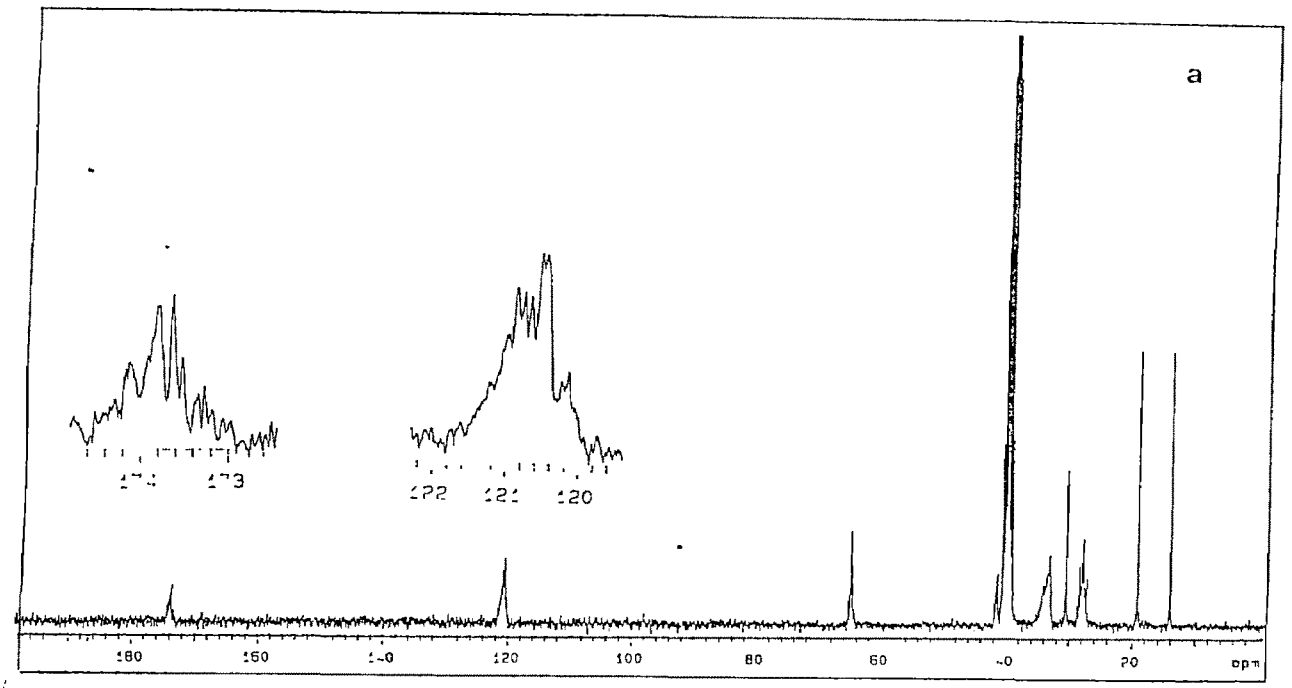

Fig.2.8 a ^{13}C NMR spectrum of $ANBA_{11}$

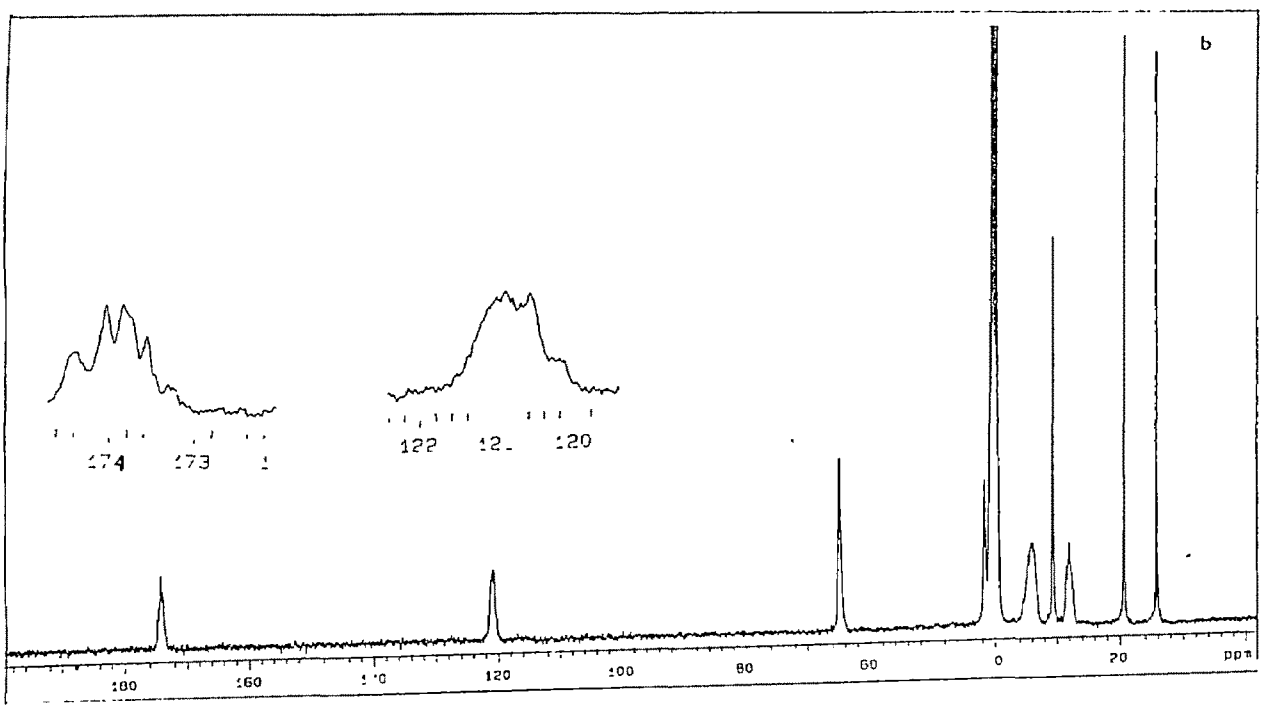

Fig.2.8 b ^{13}C NMR spectrum of $ANBA_{12}$

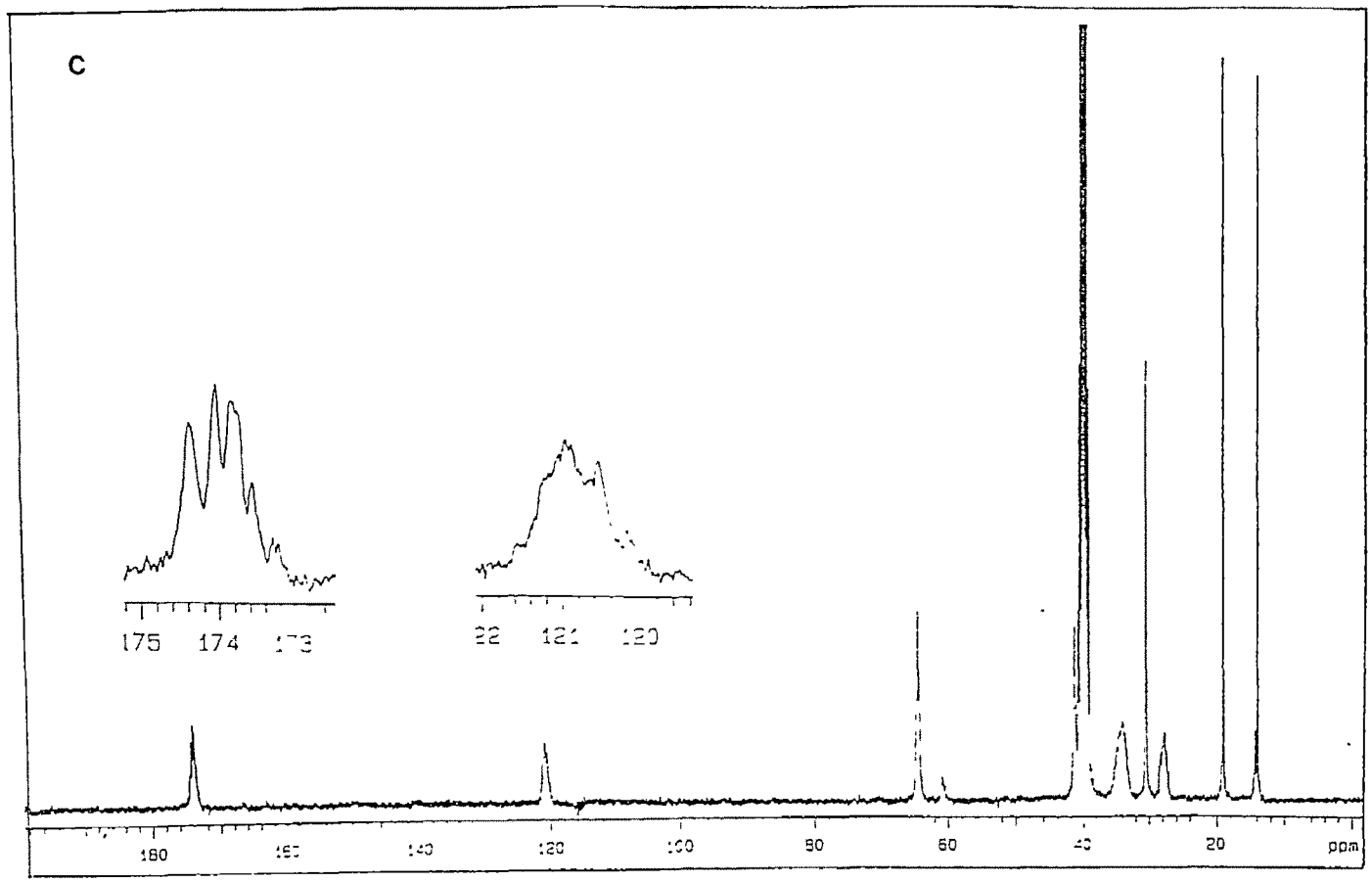

Fig.2.8 c ^{13}C NMR spectrum of $ANBA_{13}$

methacrylate - alkyl acrylate /222/, where the resolution of the carbonyl region diminished with the increasing concentration of alkyl acrylate content.

These results indicate that the incorporation of lower alkyl acrylates as in ANMA and ANEA, the tendency for ordered arrangement is relatively more with the isotactic fractions predominant. The tendency is less when higher alkyl acrylate is used as in ANBA copolymers.

2.3.4 DIFFERENTIAL SCANNING CALORIMETRY (DSC)

Figures (2.9 a,b,c,d) are the representative DSC curves of the copolymers. The heating rate was maintained at 10°C/min. The observed glass transition (Tg) are tabulated in Table 2.2. It can be seen that as the acrylate content increases, the Tg values decrease and a similar effect was also observed with higher homologous of acrylates. The glass transition temperature of PAN and polyacrylates have been reported by many workers /203, 204, 246, 247/. These values are in between those of the corresponding homopolymers.

Many Scientists /248-250/ have studied the thermal reactions of polyacrylonitrile in detail by various thermal analytical techniques and Hay /251/ has discussed the DSC curves. He reported a sharp exothermic peak at 265°C in N_2 atmosphere. Our sample also showed the same feature at 265.6°C (Fig. 2.9e), and then decomposed at higher temperature.

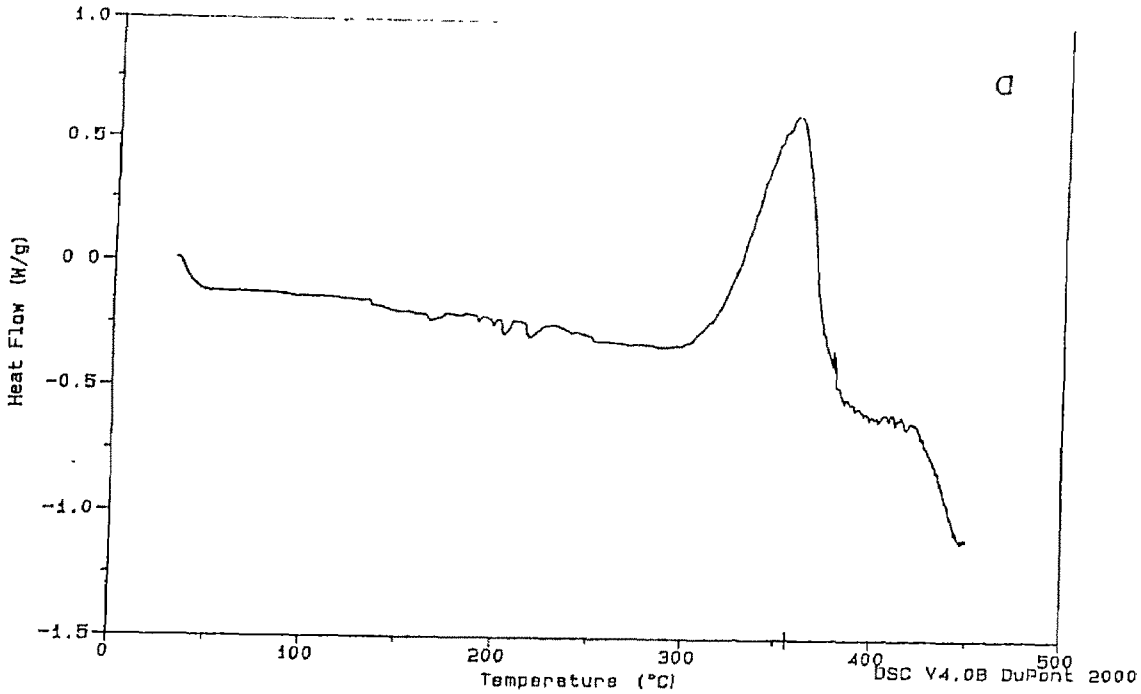

Fig.2.9 a DSC curve of $ANMA_{11}$

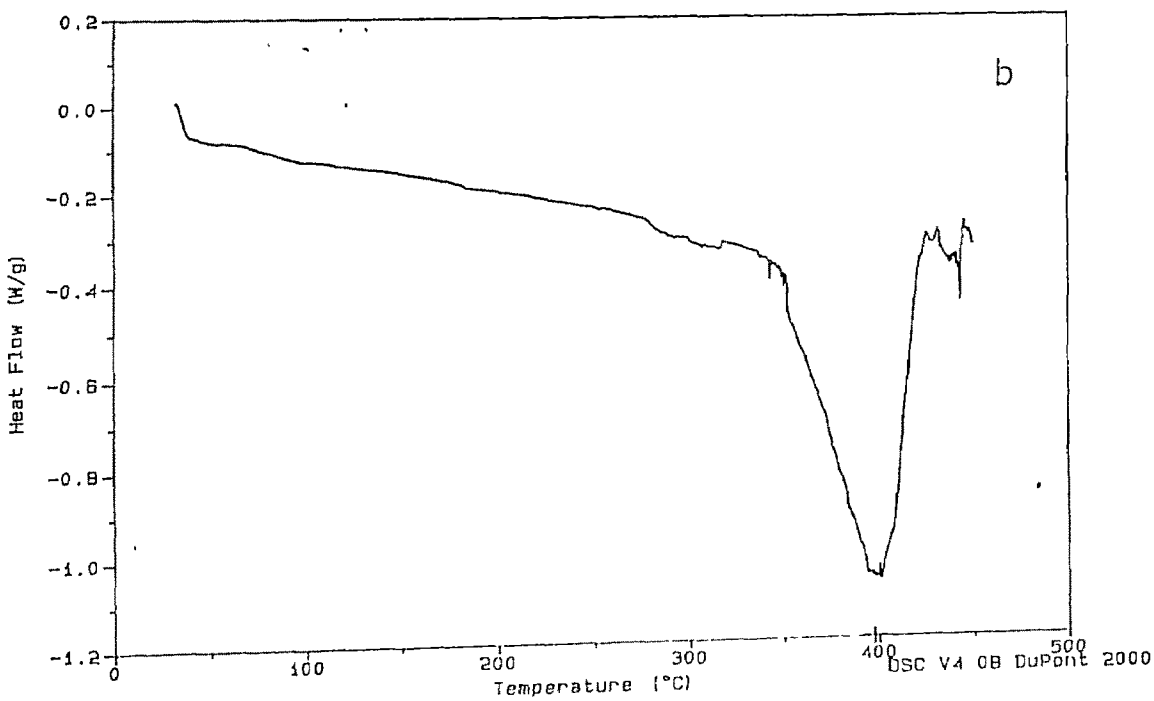

Fig.2.9 b DSC curve of $ANMA_{13}$

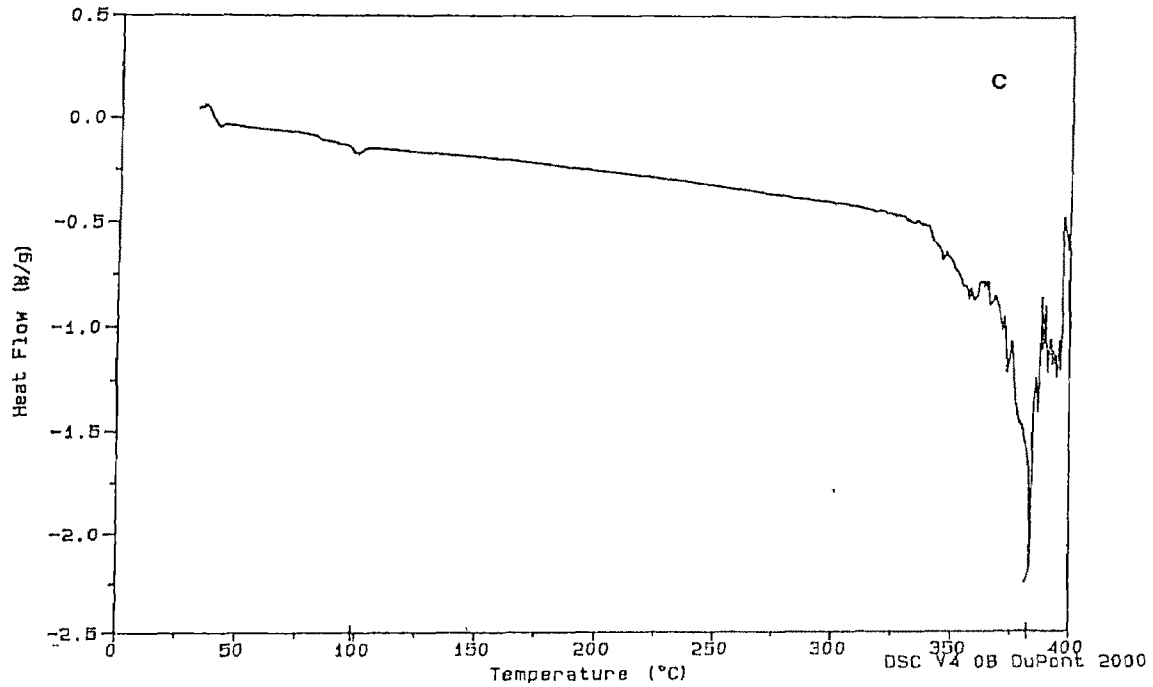

Fig.2.9 c DSC curve of $ANEA_{13}$

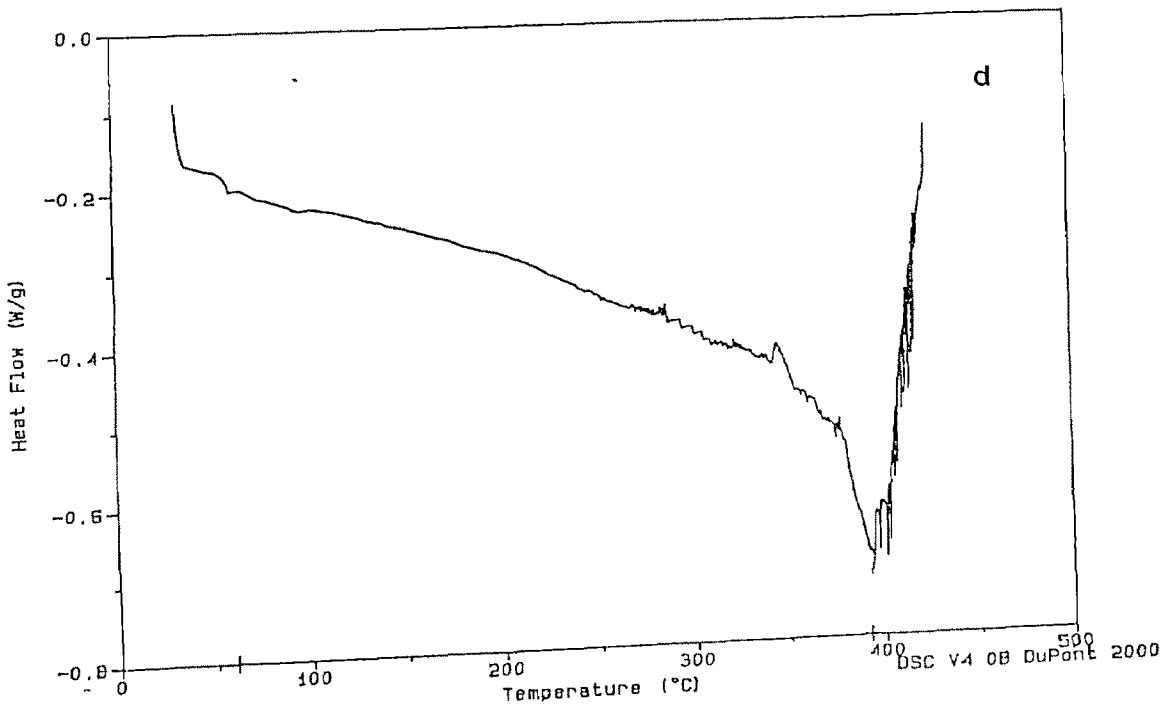

Fig.2.9 d DSC curve of $ANBA_{12}$

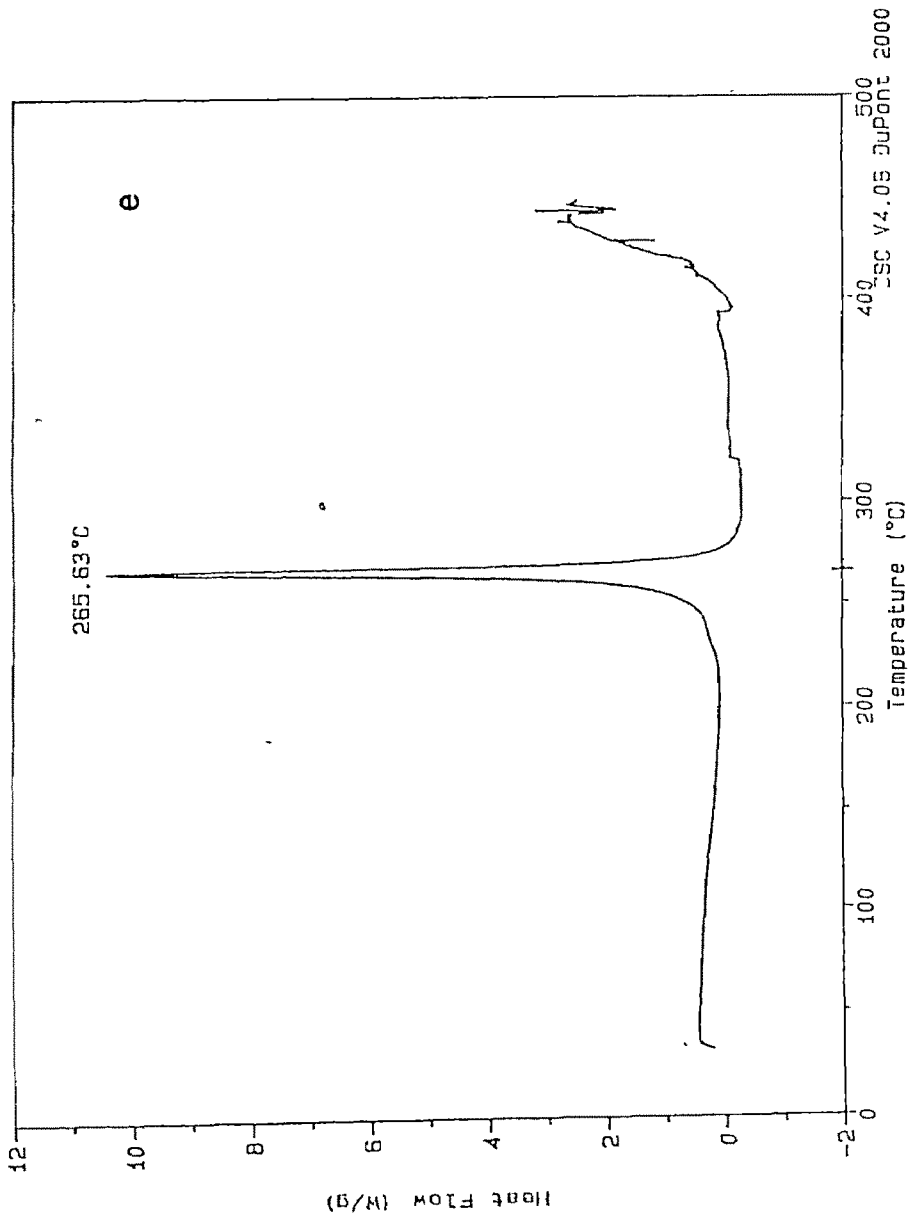

Fig.2.9 e DSC curve of PAN

The exothermic peaks were prominent only in the $ANXA_{11}$ copolymer samples. At higher acrylate concentration the exotherms were masked by the endothermic degradation process, hence the exotherms were absent. Similar observation was reported earlier /252/ in the copolymers of acrylonitrile and methyl methacrylate, where the increasing concentrations of methyl methacrylate masked the exothermic reaction. This could be attributed to the effect of the bulkier comonomer acrylates, diminishing the crystallization considerably by restricting the chain length which allows cocrystallization /252/. The decomposition endotherm sets in at a lower temperature with higher alkyl acrylate concentration. Moreover, as the molecular weight of the copolymers are not high, (Table 2.2) the large number of chain ends do not permit close packing, inducing more flexibility by occupying large free volume.

2.3.5 DIFFERENTIAL THERMAL ANALYSIS

Representative DTA, thermograms are shown in fig. 2.10 a,b,c,d. Pronounced heat changes are observed in the degradation reactions of the polymers. The exotherm starts at a higher temperature (above 400°C) in all systems indicating that the oxidative resistance of the polymers are high. As the thermal characteristics depend on the conditions under which the polymers are tested, care was taken to maintain identical experimental conditions for all the samples.

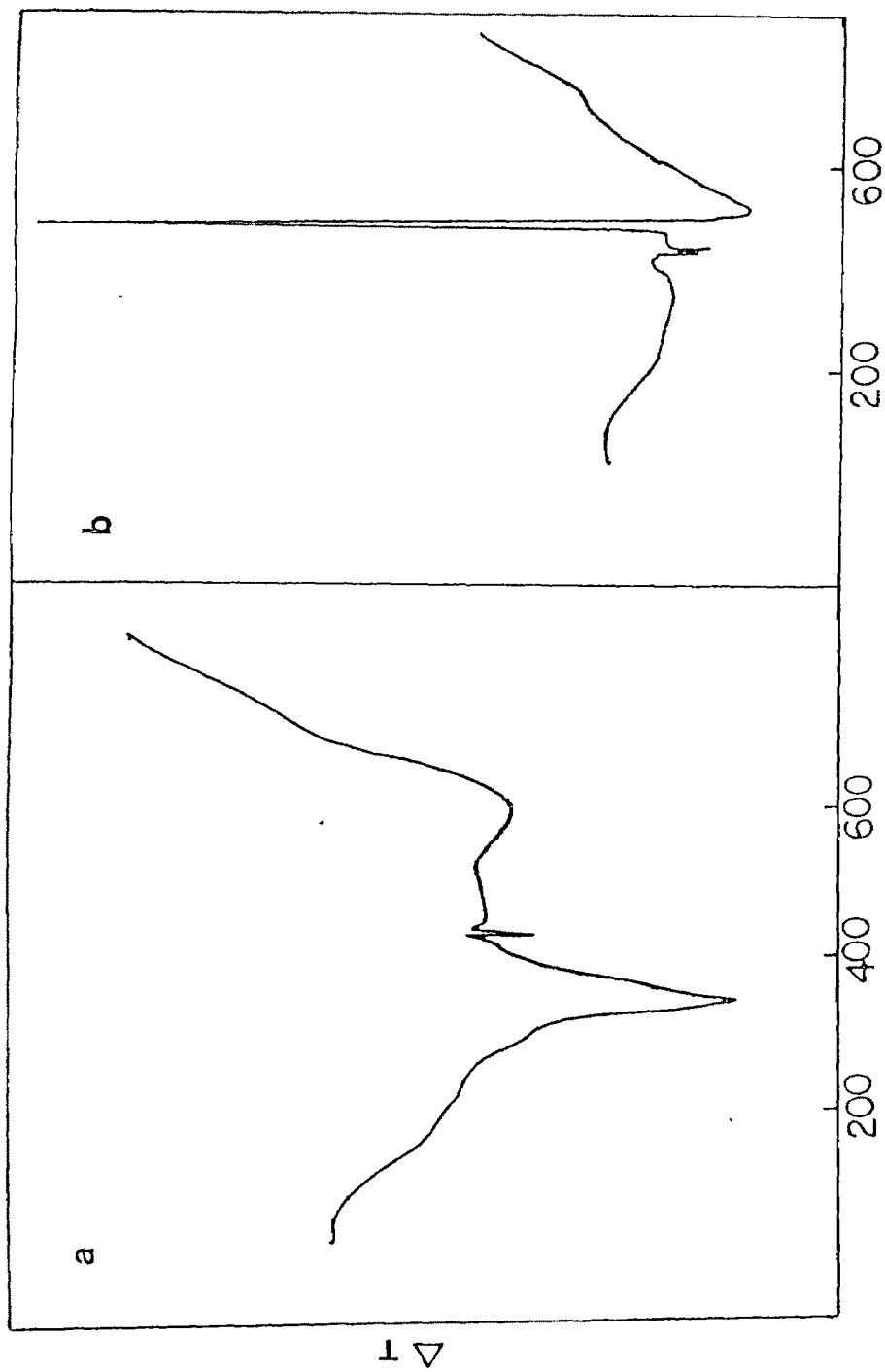

Fig. 2.10 a : DTA Thermogram of PAN Fig 2.10 b : DTA Thermogram of PBA

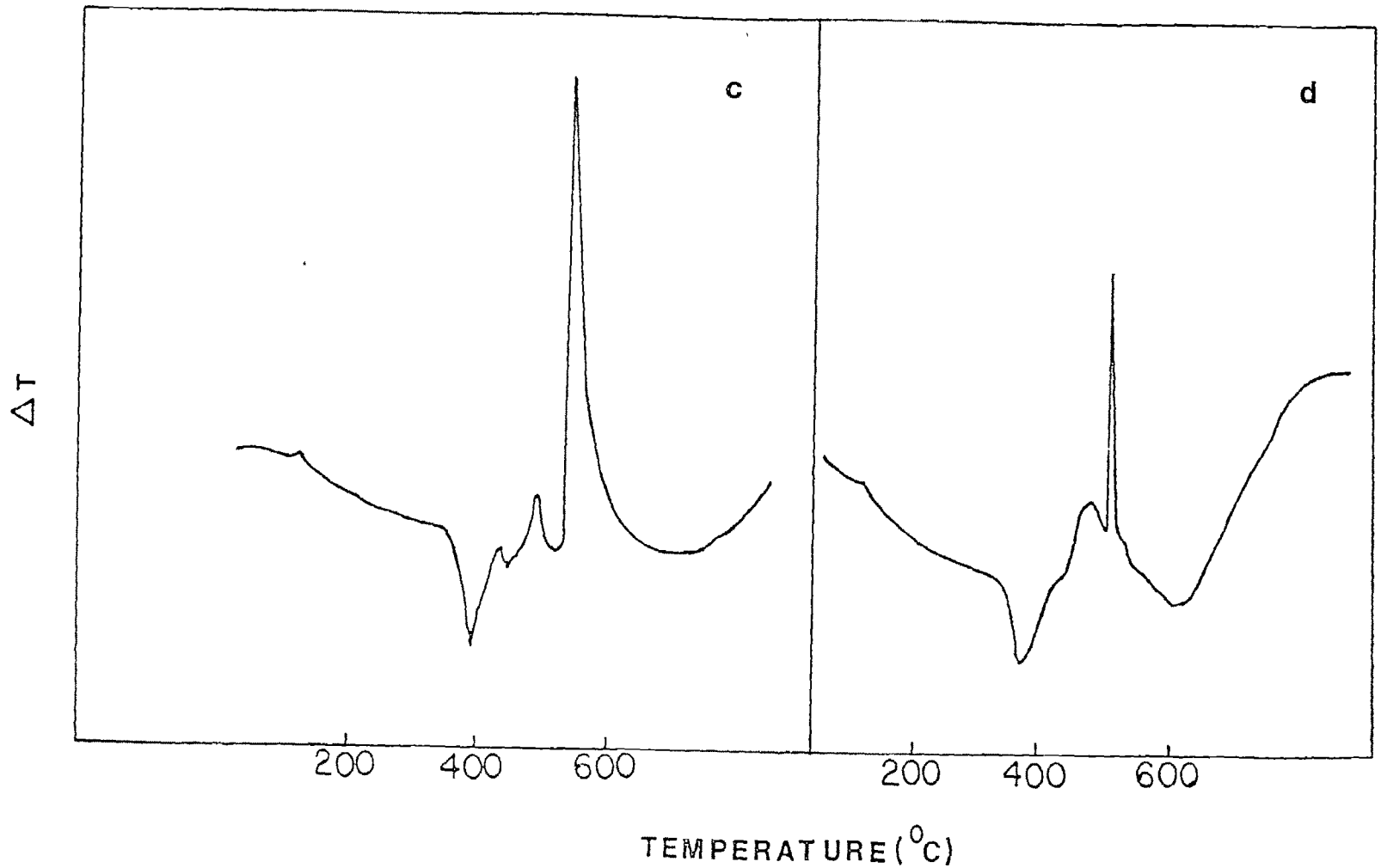

Fig. 2.10 C : DTA Thermograms of $ANBA_{11}$

Fig 2.10 D : DTA Thermograms of $ANMA_{11}$

The characteristics of DTA thermograms of PAN has been discussed by Grassie et al. /253/ in detail. The thermograms obtained shows broad shoulders. This is because the runs were performed in air. A prominant exotherm peak (very sharp) at the higher temperature region has been observed for all the copolymers and homopolymers of acrylates. This is due to the cross linking reactions taking place in the acrylate chains at the higher temperature region.

2.3.6 THERMOGRAVIMETRIC ANALYSIS (TGA)

Representative thermograms for the homopolymers and copolymers are shown in fig. 2.11 and 2.12. A different degradation mechanism for the copolymers are evident from the two stage thermograms obtained. For homopolymers the thermograms show a single step degradation pattern. Various methods /254-260/ are available for the analysis of the data. In this study the Broido method /261/ has been used to calculate the activation energy of degradation for all the systems. The equation used for the calculation of activation energy (E_a) is

$$\ln (x/y) = -(E_a/R)\ 1/T + \text{Constant} \qquad \ldots\ldots\ 2.1$$

$$\text{where } y = \frac{W_t - W_\alpha}{W_o - W_\alpha}$$

y = fraction of the number of initial molecules not decomposed.

W_t = Weight at any time t and

W_α = Maximum weight loss.

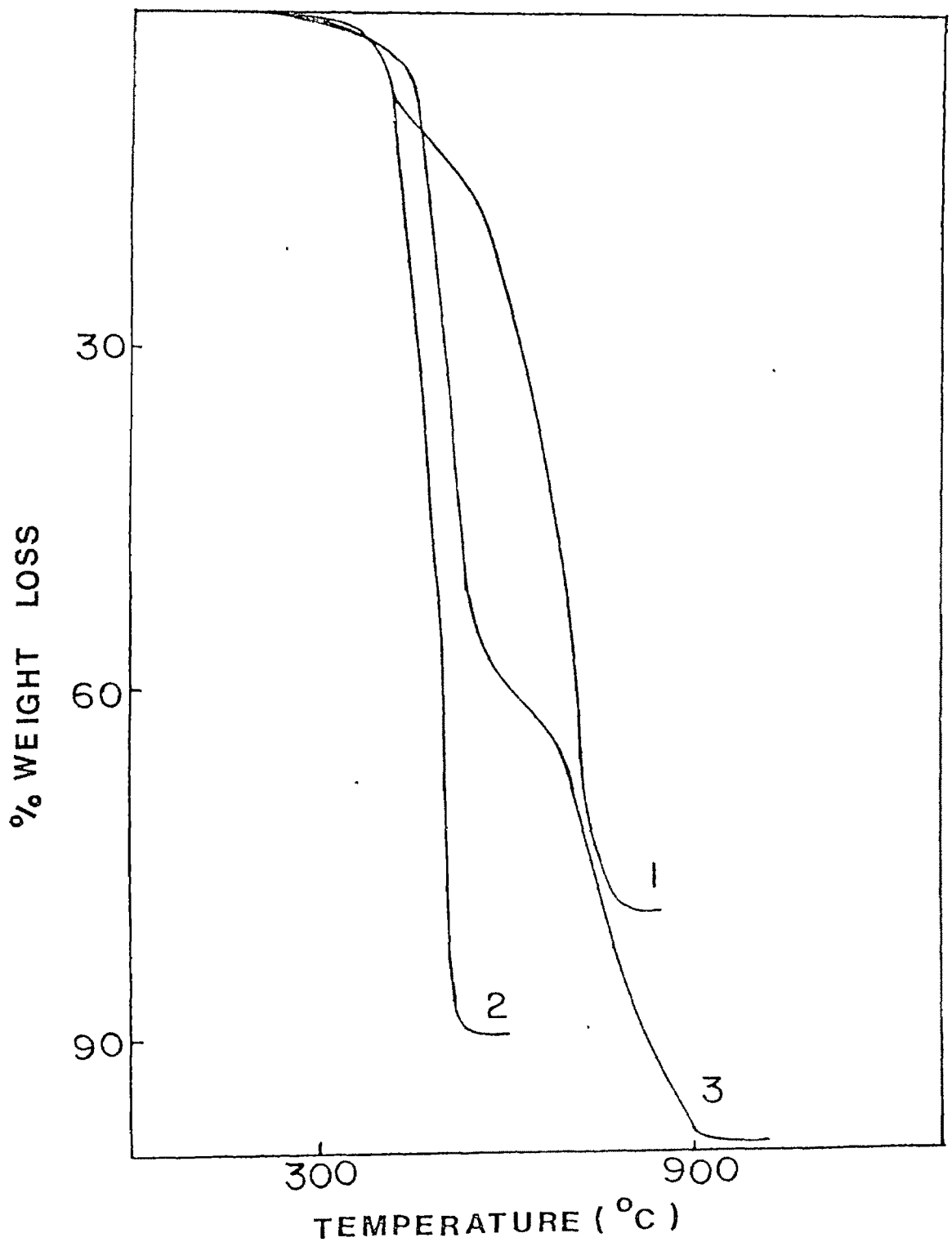

Fig. 2.11 : TGA Curve of 1. PAN 2. PBA 3. $ANEA_{11}$

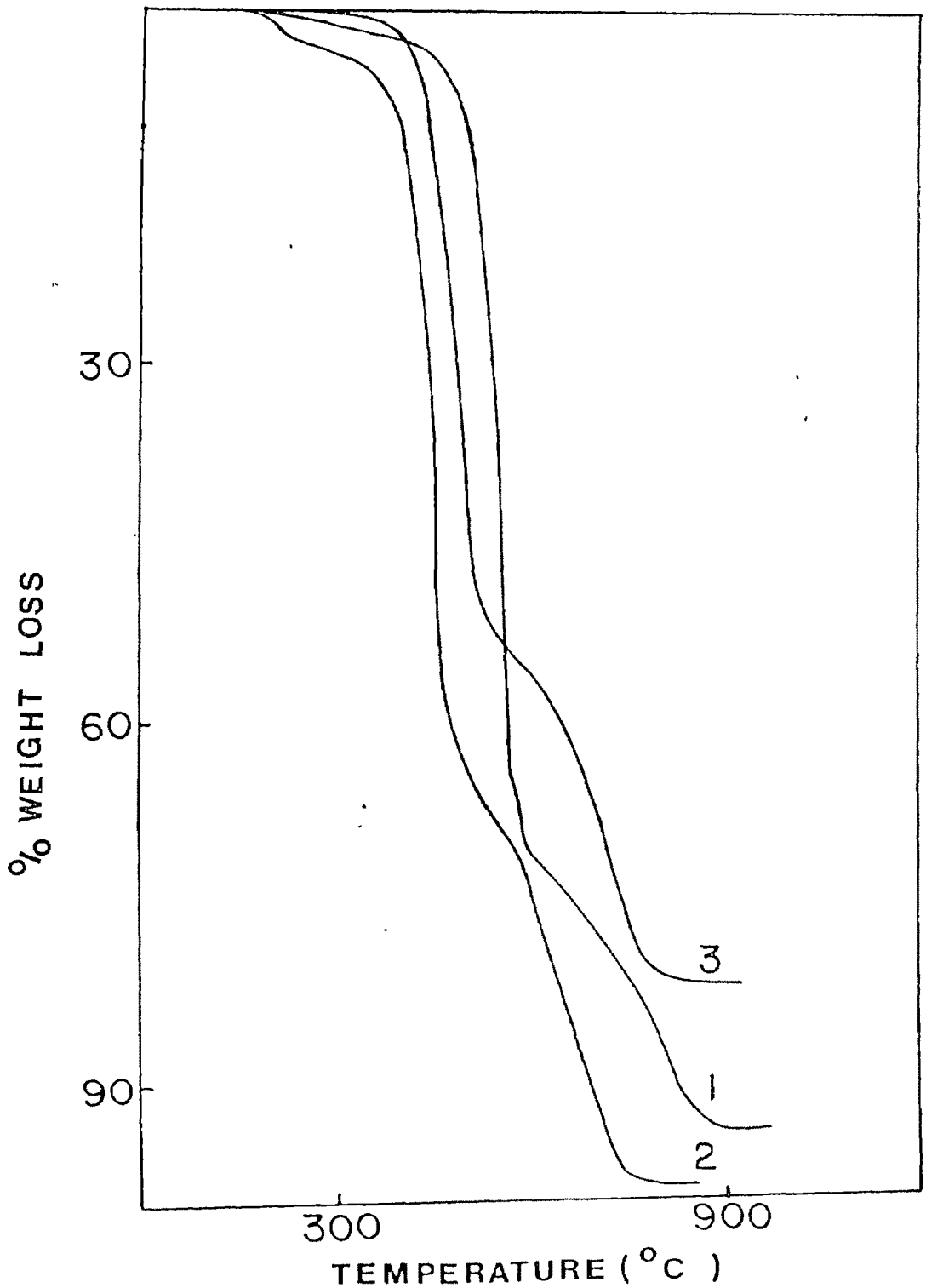

Fig. 2.12 : TGA curve of 1. $ANMA_{13}$ 2. $ANMA_{12}$ 3. $ANBA_{12}$

In equation 2.1 plot of ln ln (1/y) vs 1/T gives an excellent approximation to a straight line with a correlation coefficient greater than 0.99. The slope of this line is related to the activation energy of degradation.

The calculated activation energy of decomposition (E_a) values are compiled in Table 2.3. It can be seen that the E_a values increase when higher alkyl acrylates are present in the copolymers. These values also increased with the increasing concentration of the acrylate comonomer. The activation energy for the first decomposition step in copolymers ranges from 82.8 to 160.1 kJ mol^{-1} and from 28.8 to 54.8 kJ mol^{-1} for the second decomposition step. This indicates that major decomposition occurs in the first step.

Thermogravimetric studies of polyacrylonitrile and polyacrylates have been extensively studied by many workers /262-264/. DiEdwardo /265/ reported that there are four main catagories of degradation reaction namely chain scission, crosslinking, hydrogonation and cyclization in PAN and the main degradation products have been identified as ammonia and hydrogen cyanide /266/. The PAN thermogram shows extensive weight loss (fig. 2.11). This indicates that chain scission reactions are also evident though the predominant reaction is formation of fused heterocyclic rings /266/. The E_a value of PAN in presence of air is much less (71.5 kJ mol^{-1}) than the reported value of 129.6 kJ mol^{-1} in N_2 /262/. In case of PMA also similar decrease was observed, the reported value being 154.7 kJ mol^{-1} in N_2 /267/.

TABLE : 2.3

ACTIVATION ENERGY OF DECOMPOSITION FOR HOMOPOLYMERS AND COPOLYMERS BY THERMOGRAVIMETRIC ANALYSIS

Polymer	Decomposition Temp. (°C) range	Weight Loss (%)	E_A (kJ mol^{-1})
$ANMA_{11}$	360 - 500 510 - 800	51 97	82.8 29.7
$ANMA_{12}$	360 - 500 540 - 750	62 98	102.0 41.8
$ANMA_{13}$	420 - 620 700 - 850	70 94	150.5 41.4
$ANEA_{11}$	440 - 570 680 - 920	58 99	120.4 54.8
$ANEA_{12}$	375 - 530 560 - 810	64 93	132.1 28.8
$ANEA_{13}$	450 - 580 630 - 815	54 83	160.1 38.9
$ANBA_{11}$	380 - 520 570 - 760	44 82	120.8 53.9
$ANBA_{12}$	410 - 520 610 - 770	51 82	143.8 35.1
$ANBA_{13}$	390 - 510 560 - 665	60 93	130.4 47.2
PMA	320 - 500	89	92.0
PEA	380 - 510	87	136.3
PBA	360 - 530	90	141.3
PAN	360 - 790	79	71.5

This is because the decomposition reactions were faster in presence of air than in nitrogen. The sample characteristics also contribute to this effect. Moreover, Broido method /261/ yielded lower values /268/ when compared to the method of Flynn and Wall /256/ and Anderson and Freeman /258/.

A recent study /269/ on the thermal characteristics of the polyacrylates showed that PMA exhibited lowest thermal stability than PEA, whereas other polymers beginning from PBA exhibited higher and approximately the same thermal stability at a heating rate of 2°C. The same polyacrylates considered in the present study also followed a similar pattern (Table 2.3). It was suggested that at higher heating rates crosslinks can not be formed as the temperature range in which crosslinking was possible, continued only for a short duration. In other words, though the crosslinking process at the initial stage of thermal degradation in PMA was thermodynamically favourable, it did not occur at high heating rate due to kinetic reasons. Hence, the observed E_a values are lower /269/.

The sharpness of decomposition indicates that the process was an autocatalytic chain reaction /270/.

2.3.7 CONTACT ANGLE

The critical surface tension (γ_c) is a useful means of determining the wetting behaviour of the polymer surface. The wettability and

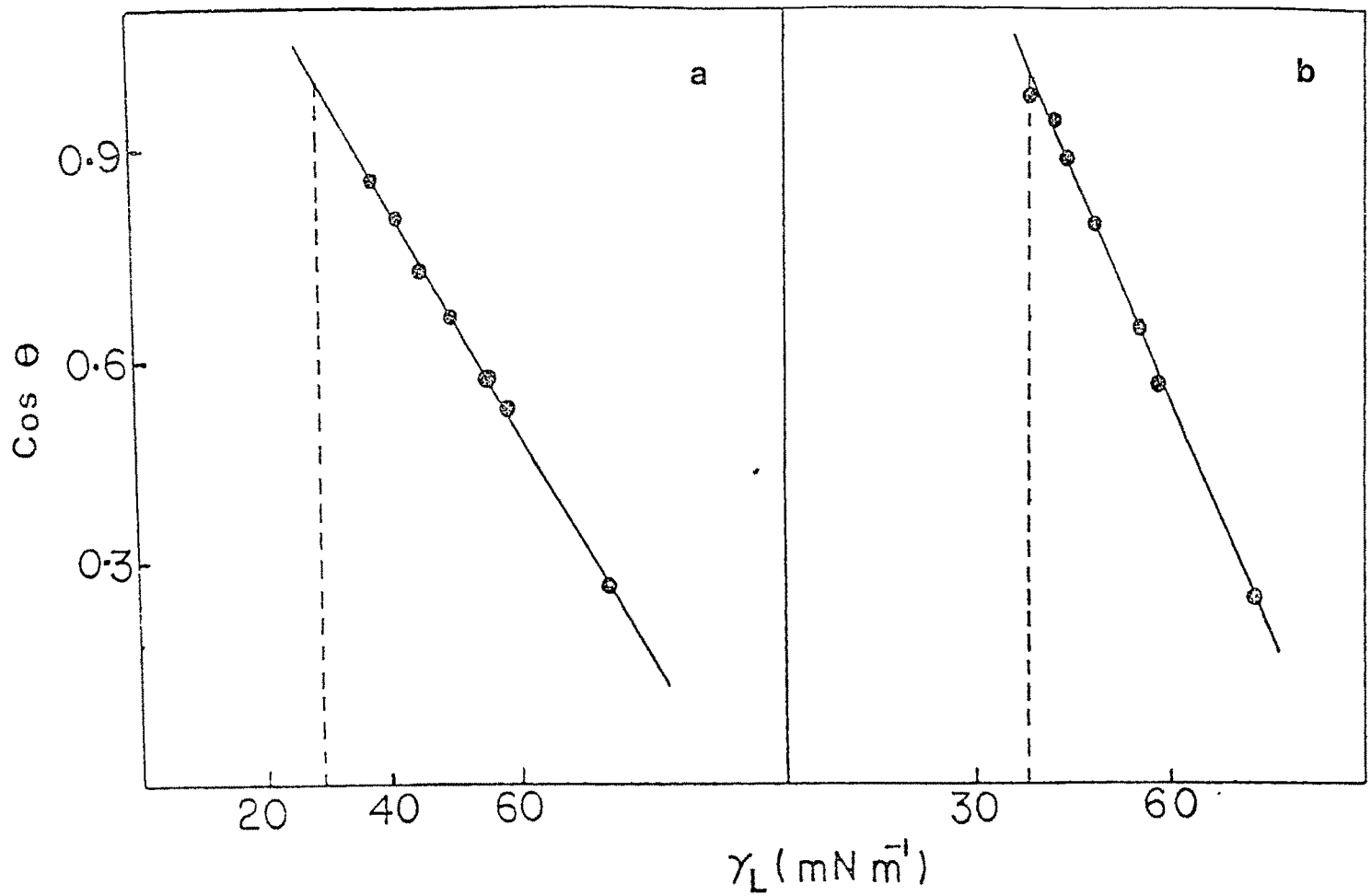

Fig. 2.13 : Plot of Cos θ against γ_L for a. $ANEA_{12}$ b. $ANMA_{11}$

structure of the polymers have been correlated by many workers /271-275/. A rectilinear relation exists between Cos Θ and surface tension of the liquids (γ_L) used, where represents contact angle of the surface with liquid. Hence the linear plot of Cos Θ Vs γ_L was extrapolated to Cos Θ = 1 to obtain the critical surface tension γ_C of the copolymers. The γ_C values are tabulated in Table 2.2. Representative plots of Cos Θ Vs γ_L are shown in fig. 2.13 a,b. This indicates that the liquids with surface tension higher than γ_C will not spread easily on the polymer surfaces. It was observed that γ_C values decreases with increasing acrylate concentration in the copolymer. Similar effect was seen with the higher homologous of acrylates. Hence it could be surmised that as the acrylate concentration is increased hydrophobicity increases in the copolymers. The γ_C values of the copolymers with 1:1 ratio of acrylate and acrylonitrile were nearer to the reported /236/ values for the poly acrylates i.e. 35 mNm^{-1}.

2.3.8 DILUTE SOLUTION VISCOSITY STUDY

Viscosity of copolymers and homopolymers were studied in NN' Dimethyl formamide at four temperatures 30°, 35°, 40° and 45°C. The intrinsic viscosities were computed by well known procedures /276/. The values are tabulated in Table 2.4. The correlation coefficient was always 0.99 or better. It can be seen that $|\eta|$ decreases as the temperature increases and $|\eta|$-T plots are linear with negative slope. A few representative plots are shown in fig. 2.14. This indicates

TABLE : 2.4

INTRINSIC VISCOSITY OF VARIOUS COPOLYMERS AND HOMOPOLYMERS AT DIFFERENT TEMPERATURES IN DIMETHYL FORMAMIDE SOLUTION

Polymer (feed ratio) g/g (AN:XA)	Expt. mole. ratio (AN:XA)	Intrinsic viscosity $\|\eta\|$ (dl g^{-1})			
		30°C	35°C	40°C	45°C
$ANMA_{11}$	1 : 0.86	0.294	0.283	0.274	0.266
$ANMA_{12}$	1 : 1.40	0.258	0.251	0.242	0.237
$ANMA_{13}$	1 : 2.27	0.249	0.240	0.229	0.221
$ANEA_{11}$	1 : 0.58	0.385	0.381	0.375	0.372
$ANEA_{12}$	1 : 0.98	0.336	0.331	0.328	0.320
$ANEA_{13}$	1 : 1.36	0.365	0.353	0.342	0.327
$ANBA_{11}$	1 : 0.52	0.295	0.289	0.281	0.275
$ANEA_{12}$	1 : 0.82	0.288	0.282	0.275	0.270
$ANEA_{13}$	1 : 0.96	0.267	0.255	0.250	0.245
PMA		0.255	0.251	0.248	0.245
PEA		0.347	0.343	0.339	0.335
PBA		0.256	0.252	0.249	0.245
PAN		0.727	0.721	0.712	0.704

AN = acrylonitrile, MA = methyl acrylate

EA = ethyl acrylate, BA = butyl acrylate

Subscripts 11, 12 and 13 signify 1g of AN and 1,2.3 g of second component in the copolymer

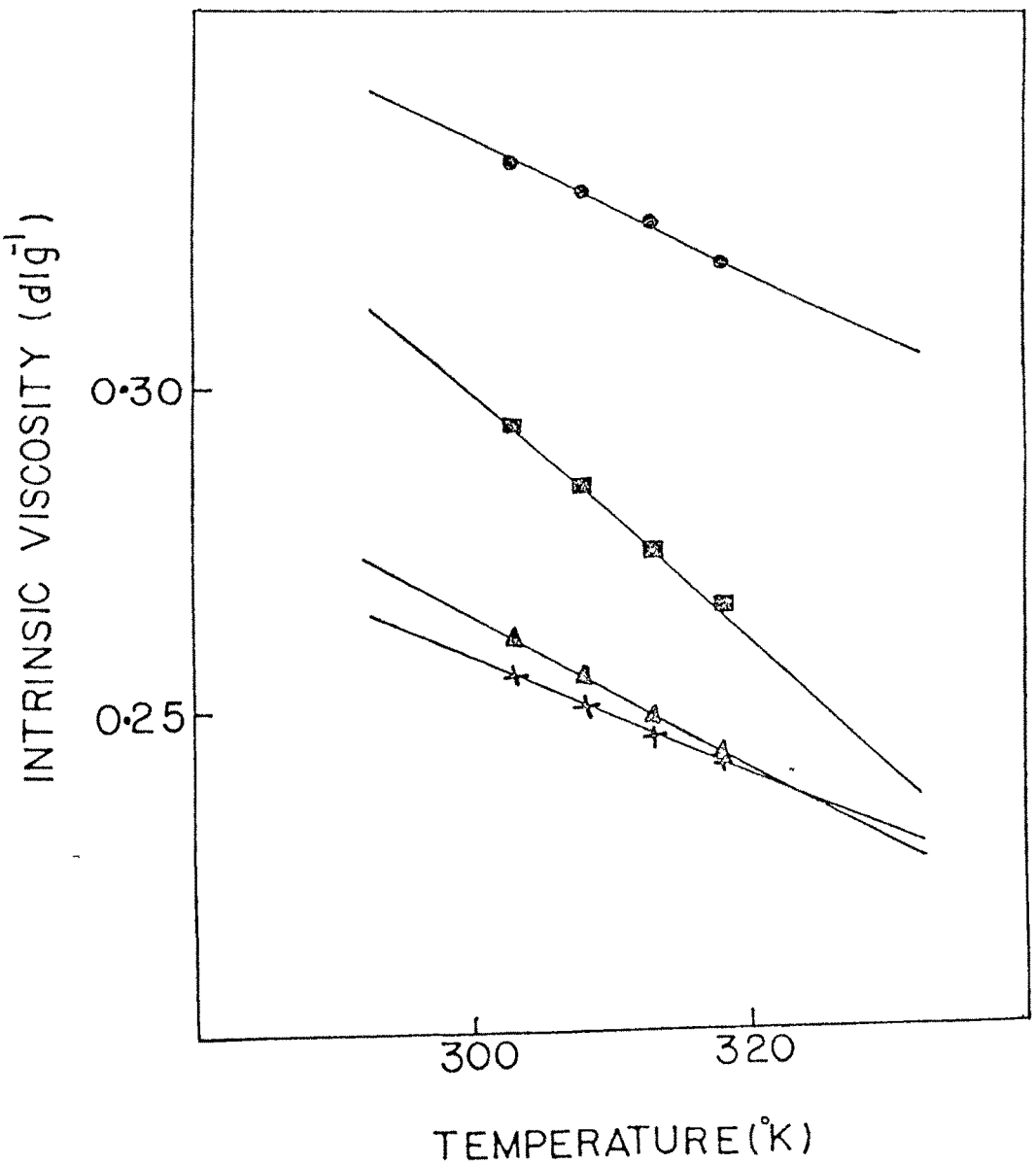

Fig. 2.14 : Plot of intrinsic viscosity (dl/g) against temperature

● $ANEA_{12}$ ■ $ANMA_{11}$ ▲ $ANBA_{13}$ X PMA

that the swelling of the polymer coils are not much in these systems and there are lower critical solution temperatures (LCST) for these polymer solutions. The intrinsic viscosity change with temperature for homopolymer solutions is similar to that for copolymer solutions. A critical look at the $|\eta|$ data shows that in general as the weight ratio of acrylonitrile decreases in the copolymers, the intrinsic viscosity also decreases at all temperatures, the only exception being for the acrylonitrile - ethyl acrylate copolymers. In this case a minimum occurs as the ratio decreases, but at higher temperatures the minimum becomes less prominent.

From the viscosity data, various activation parameters of the viscous flow were evaluated using Frenkel - Eyring /277/ equation.

$$|\eta| = (Nh/V) \exp (\triangle G^{\ddagger}_{vis}/RT) \qquad \ldots\ldots 2.2$$

Where V is the molar volume of the solution, N is Avogadro's number, h is Plank's constant, R is the gas constant, T is temperature$\overset{(K)}{\wedge}$ and $\triangle G^{\ddagger}_{vis}$ is the activation free energy for the viscous flow.

This equation can be rewritten as

$$\ln (\eta V/Nh) = \triangle G^{\ddagger}_{vis}/RT = \triangle H^{\ddagger}_{vis}/RT - \triangle S^{\ddagger}_{vis}/R \qquad \ldots\ldots 2.3$$

Where $\triangle H^{\neq}_{vis}$ and $\triangle S^{\neq}_{vis}$ are the activation enthalpy and entropy changes for the viscous flow.

ln (ηV/Nh) was plotted against T^{-1} and was found to be linear for all the systems. The slope and intercept gave $\triangle H^{\neq}_{vis}$ and $\triangle S^{\neq}_{vis}$ respectively. Some representative plots are given in fig. 2.15. $\triangle G^{\neq}_{vis}$, $\triangle H^{\neq}_{vis}$ and $\triangle S^{\neq}_{vis}$ are compiled in Table 2.5. V is the molar volume of the solution, but the molar volume of a polymer solution is an enigma and hence the molar volume of the solvent was used in the calculations because the densities of the polymer solution and that of the solvent are generally same /278/. In all systems $\triangle H^{\neq}_{vis}$ and $\triangle S^{\neq}_{vis}$ are constant quantities, independent of temperature, which signifies that the systems are not crosslinked. It is also observed that the heats of activation of viscous flow are generally positive and decreases as the concentration of the polymer in solution decreases (Table 2.6). The values are not large, the highest value observed was around 10 kJ mol^{-1} for PAN at 0.8 g/dl concentration. The entropies of activation of viscous flow process are low and negative, indicating that the polymer structures are poorly ordered in this solvent system. Although there seems to be a decrease in $\triangle S^{\neq}_{vis}$ for almost all the systems as a function of polymer concentration with the exception of PAN, the changes are not significant and atleast in these polymer systems it can be safely assumed that $\triangle S^{\neq}_{vis}$ is constant independent of composition and concentration. From the free energy values in Table 2.5 it can be seen that $\triangle G^{\neq}_{vis}$ is independent of temperature and is similar for all the systems.

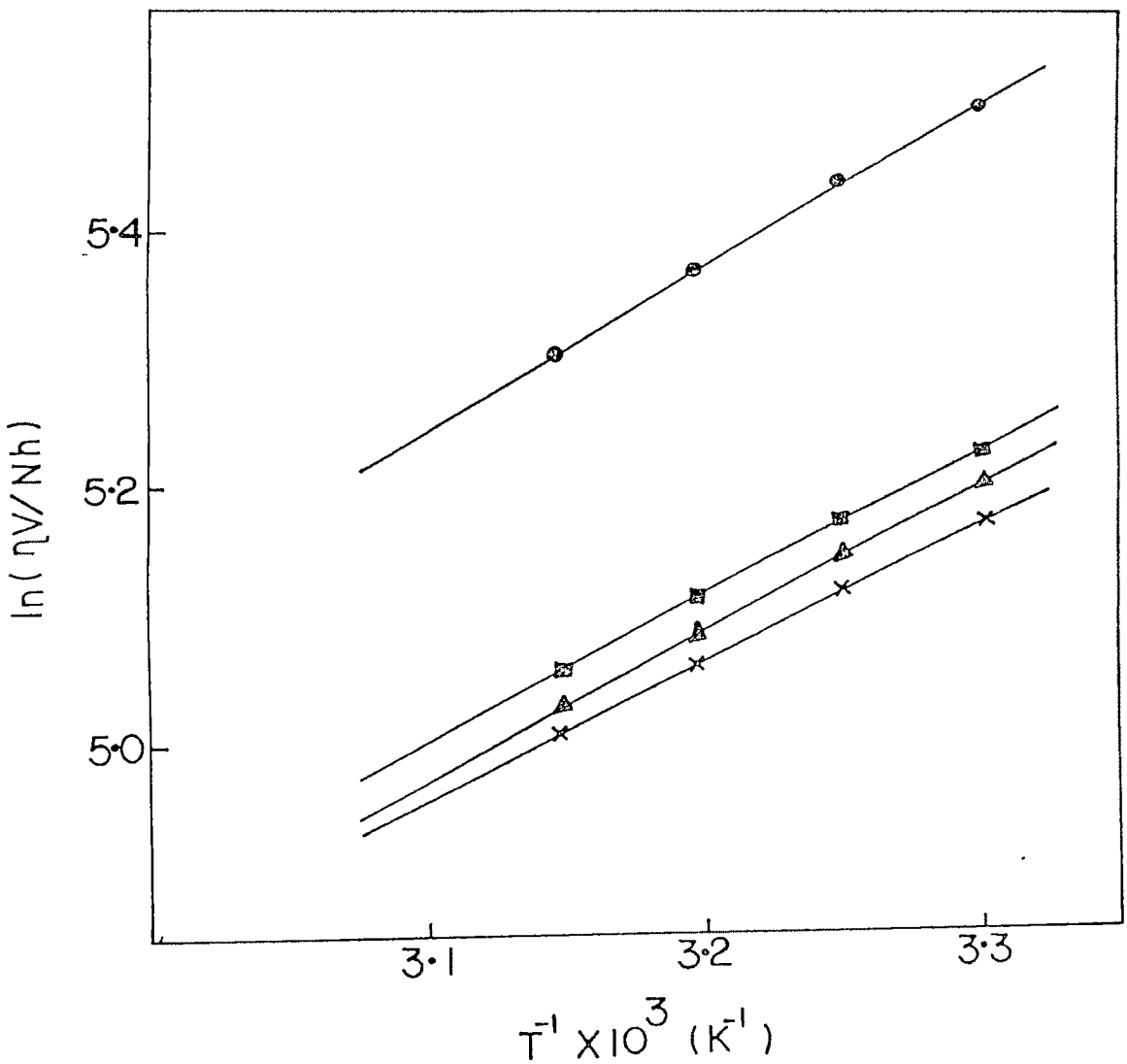

Fig. 2.15 : Plot ln ($\eta V/Nh$) vs T^{-1}

● PAN ■ $ANEA_{12}$ ▲ $ANMA_{11}$ X $ANBA_{13}$

TABLE : 2.5

FREE ENERGY $\triangle G^{\ddagger}_{vis}$, ENTHALPY $\triangle H^{\ddagger}_{vis}$ AND ENTROPY $\triangle S^{\ddagger}_{vis}$ OF ACTIVATION FOR THE VISCOUS FLOW OF THE POLYMERS IN DIMETHYL FORMAMIDE (0.8 g/dl) SOLUTION

Polymer	$\triangle G^{\ddagger}_{vis}$ (kJ mol^{-1})				$\triangle H^{\ddagger}_{vis}$	$-\triangle S^{\ddagger}_{vis}$
	30°C	35°C	40°C	45°C	(kJ mol^{-1})	(J $mol^{-1}K^{-1}$)
$ANMA_{11}$	13.1	13.2	13.2	13.3	9.4	12.3
$ANMA_{12}$	13.1	13.1	13.2	13.3	9.2	12.9
$ANMA_{13}$	13.0	13.1	13.2	13.3	8.9	13.6
$ANEA_{11}$	13.3	13.4	13.4	13.5	9.4	13.0
$ANEA_{12}$	13.2	13.3	13.3	13.4	9.1	13.6
$ANEA_{13}$	13.2	13.3	13.4	13.4	9.6	12.1
$ANBA_{11}$	13.1	13.2	13.3	13.3	9.0	13.7
$ANBA_{12}$	13.1	13.2	13.2	13.3	9.1	13.3
$ANBA_{13}$	13.1	13.1	13.2	13.2	9.0	13.3
PMA	13.0	13.1	13.2	13.3	8.9	13.8
PEA	13.2	13.3	13.3	13.4	8.9	14.0
PBA	13.1	13.1	13.2	13.3	9.0	13.5
PAN	13.9	13.9	14.0	14.1	10.4	11.4

TABLE : 2.6

FREE ENERGY $\triangle G^{\neq}_{vis}$, ENTHALPY $\triangle H^{\neq}_{vis}$ AND ENTROPY $\triangle S^{\neq}_{vis}$ FOR THE VISCOUS FLOW AT 30°C WITH VARIOUS CONCENTRATION OF POLYMER $ANMA_{11}$

Concentration of polymer soln. (g dl^{-1})	$\triangle G^{\neq}_{vis}$ (kJ mol^{-1})	$\triangle H^{\neq}_{vis}$ (kJ mol^{-1})	$-\triangle S^{\neq}_{vis}$ (J $mol^{-1} K^{-1}$)
0.8	13.11	9.4	12.32
0.6	12.95	9.2	12.48
0.48	12.89	9.0	12.88
0.40	12.81	8.9	12.90
0.20	12,.71	8.8	12.96

The Frenkel - Eyring equation of viscous flow has also been written as /279/

$$\eta = A \exp (\triangle G^{\neq}_{vis} / RT) \qquad \ldots\ldots 2.4$$

Where the pre exponential factor A was difficult to determine. It has been suggested though that A is approximately equal to 10^{-3} poise /280/. Comparing this equation with 2.2 it is clear that A$\simeq$ (Nh/V). Using appropriate units it is calculated that Nh itself is approximately equal to 10^{-3} poise, signifying that the molar volume is 1 ml. This seems to be unlikely and hence it is suggested that equation 2.2 should always be used to compute the activation parameters of viscous flow with V as the molar volume of the solvent.

The relative viscosity data at any concentration, η_r, helps in calculating the voluminosity V_E of polymer solutions. Recently, it has been used to determine the shape of protein molecules in solution /281/. V_E was calculated by plotting Y against C where C is concentration in g/ml and

$$Y = (\eta_r^{0.5} - 1) / [C (1.35 \eta_r^{0.5} - 0.1)] \qquad \ldots\ldots 2.5$$

The plot was linear and was extrapolated to C = 0 (Fig. 2.16) and V_E was obtained from the intercept. Voluminosity (ml/g) at infinite dilution is a function of temperature and is a measure of the volume of the solvated polymer molecules.

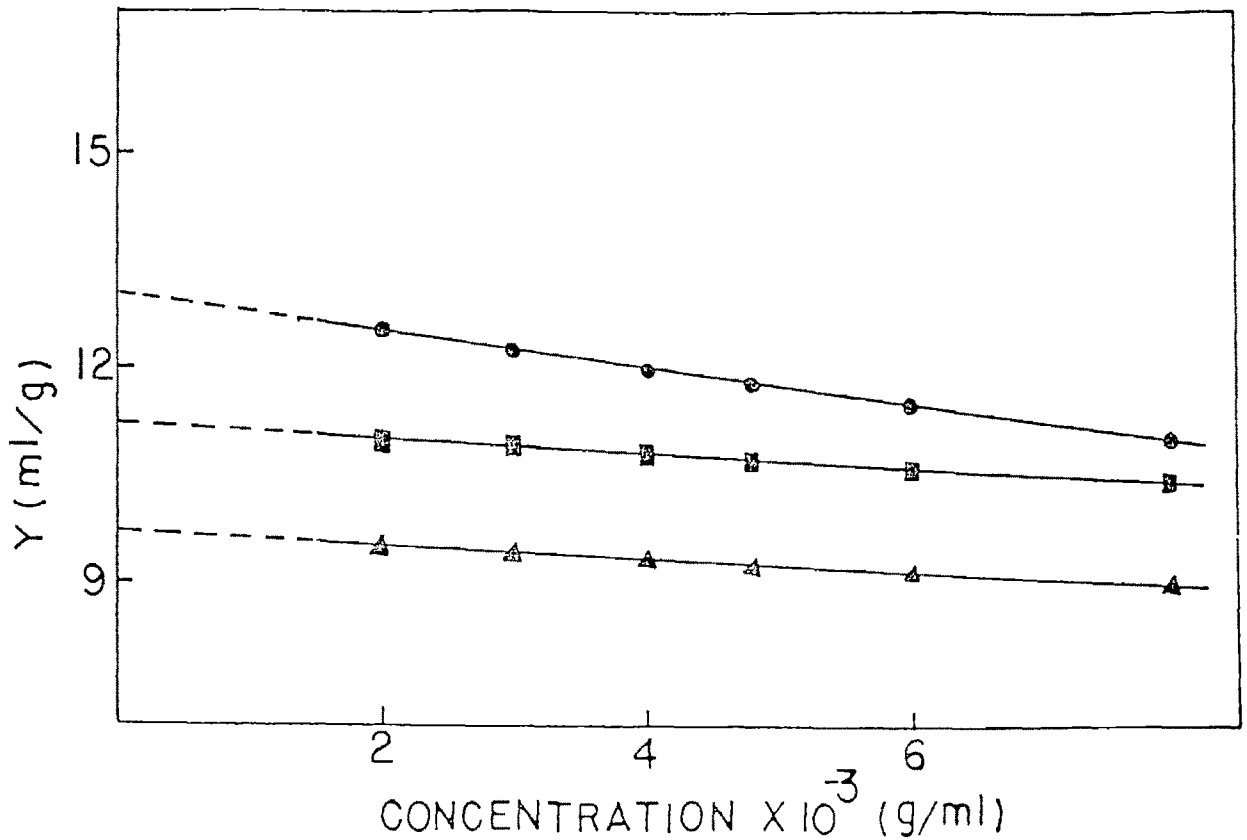

Fig. 2.16 : Plot of Y vs concentration (g/ml) where
$Y = (\eta_r^{0.5} - 1) / [C(1.35\ \eta_r^{0.5} - 0.1)]$

● $ANEA_{12}$ ▣ $ANBA_{11}$ ▲ $ANMA_{12}$

TABLE : 2.7

VOLUMINOSITY V_E AT DIFFERENT TEMPERATURES AND THE SHAPE FACTOR ν at 40°C

Polymer	V_E (ml g^{-1})				ν 40°C
	30°C	35°C	40°C	45°C	
$ANMA_{11}$	11.68	11.29	10.92	10.62	2.51
$ANMA_{12}$	10.32	9.97	9.70	9.46	2.49
$ANMA_{13}$	9.95	9.58	9.30	8.99	2.46
$ANEA_{11}$	15.35	14.99	14.62	14.48	2.56
$ANEA_{12}$	13.39	13.30	13.00	12.97	2.51
$ANEA_{13}$	14.45	14.16	13.60	12.99	2.51
$ANBA_{11}$	11.74	11.54	11.20	11.04	2.51
$ANBA_{12}$	11.46	11.18	10.90	10.78	2.52
$ANBA_{13}$	10.30	10.16	9.95	9.69	2.51
PAN	28.27	27.72	27.05	26.85	2.55
PMA	10.19	9.95	9.90	9.69	2.50
PEA	13.64	13.51	13.40	13.25	2.52
PBA	10.81	10.01	9.90	9.78	2.51

The intrinsic viscosity

$$| \eta | = \nu V_E \qquad \ldots\ldots 2.6$$

where ν is the shape factor /282/. The shape factor is a quantity which gives an idea about the shape of the molecules in solution. If it is 2.5, the molecules are spherical in shape. If the molecules in solution are oblate or prolate /283,284/ the values are different. For all the systems at all temperatures considered for this study ν was found to be 2.5 (Table 2.7) indicating that in dilute solutions the copolymers of acrylonitrile and acrylates are spherical in nature.

As the temperature increases the solvation decreases and hence V_E decreases. This decrease is linear though the rates of changes are different. This indicates that the effect of temperature on the polymer - solvent interaction is different. Moreover, in general the higher the amount of acrylate in the copolymer lesser is the solvation. Hence it can be concluded that the polymer - solvent interaction is affected by the copolymer composition, temperature etc., although the conformation of the polymer molecules in dimethyl formamide solution is spherical at all temperatures regardless of the amount of acrylate and type of acrylate present.